Stress Relaxation Under Various Stress and Drainage Conditions

Gilberto Alexandre, Ian Martins

Stress Relaxation Under Various Stress and Drainage Conditions

Gilberto F. Alexandre, D.Sc.
Ian S. M. Martins, D.Sc., Associate Professor COPPE/UFRJ

Abstract

This paper presents predictions made for stress relaxation tests carried out by Garcia (1996) in the edometric apparatus in a soft organic clay from Rio de Janeiro, Brazil. The predictions were made based on the framework of the model developed by Martins (1992), as modified by Alexandre (2006), and in agreement with concepts and ideas developed by Terzaghi (1941), Taylor (1942) and others. The differential equation of the stress relaxation test, its solution, the assessment of the parameters of the model as well as predictions made for all tests are shown in this paper. It is shown that satisfactory agreement between predictions and tests results were obtained for the soft clay tested by Garcia (1996). In addition, discussions about stress relaxation tests carried out under different conditions (triaxial and hydrostatic) and about the variation of K_0 during stress relaxation and secondary consolidation are also presented in this paper.

Keywords

Stress relaxation. Constitutive equations. Soil behavior. Rate effects. Time Effects. Viscosity. Adsorbed water layer. K_0.

Introduction

Concrete, steel, wood and glass as well as soils and rocks, among other materials, present stress relaxation.

In general terms, stress relaxation is the decrease of stress with time at constant strain and temperature and, according to Sheahan (1998), it is the least understood of the time effects in soils. Nevertheless, understanding stress relaxation is important, as for example, Coulomb's law of friction for soils depends on the normal effective stress. In addition, it would be interesting to know if horizontal stresses vary in time behind rigid restrained retaining walls. The understanding of stress relaxation is also important because it adds to the understanding of the general behavior of the soil.

The study presented herein deals with the stress relaxation of saturated clays under various stress conditions as well as under drained and undrained conditions. In more specific terms, this study aims at answering the following questions regarding the stress relaxation of a saturated clay:

- What is the mechanism behind the decrease in stress with time?
- Is there an end for stress relaxation? and;
- How stress relaxation progresses with time?

To answer these questions, the model developed by Martins (1992) for saturated normally consolidated clayey soils, as modified by Alexandre (2006), is used.

Regarding the predictions presented in this paper for the stress relaxation tests carried out by Garcia (1996) in the edometer apparatus, it must be mentioned that they are not really true predictions as they were made after the execution of the tests. In addition, the results of these tests were used for deriving the parameters of the model. Nevertheless, they are predictions in the sense that they are not fittings to the experimental stress relaxation data.

The next section presents a brief description of works carried out by other investigators regarding stress relaxation, followed by the introduction of basic concepts of Martins's Model and the analytical study of the stress relaxation. Subsequently, the parameters of the model are derived and predictions are made for the tests carried out by Garcia (1996). Closing this paper, a comparison between the predictions and tests, discussions and considerations regarding various other stress and drainage conditions, and the variation of K_0 during stress relaxation and secondary consolidation in the edometer are presented.

Previous Studies and Approaches

It seems that Taylor (1943) was the first investigator to carry out stress relaxation tests in the triaxial apparatus. In Taylor (1955), data from 13 stress relaxation tests carried out during the final stages of shear tests on the Boston Blue Clay are presented. By using a proving ring in the tests the investigator was able to assess strain rates during the execution of the tests.

Among the tests reported in Taylor (1955), Tests 26 and 28 are specially worth commenting on. Test 26 lasted for about 3,600 minutes reaching a strain rate of about $9x10^{-6}$ %/min when it was terminated and presented a decrease in the deviatoric stress of about 31%. On the other hand, Test 28 reached a strain rate of about $1.2x10^{-5}$ %/min when it was terminated and presented a decrease in the deviatoric stress of about 27%. More importantly, differently from Test 26, in Test 28, the deviatoric stress seamed to have reached a stationary value. Also according to Taylor (1955), the decrease in shearing strength for the Boston Blue Clay was about 9% per log cycle.

Other investigators that carried out stress relaxation tests in the triaxial apparatus comprise Saada (1962), Wu et al. (1962), Murayama and Shibata (1964), Lacerda and Houston (1973), Murayma et al. (1974), Akai et al. (1975), Hicher (1988), Silvestri et al. (1988) and Sheahan (1991). In general, what is observed during stress relaxation is that the deviatoric stress decreases through time until a stationary value is reached and that pore-pressures decrease slightly. Representing time in the horizontal axis in a log scale and the deviatoric stress in the vertical axis, the deviatoric stress x time (log scale) curve in most relaxation tests present an initial convex portion that is followed by what appears to be approximately a straight line.

Apart from tests carried out in the triaxial apparatus under deviatoric stresses, other types of stress relaxation tests were carried out by other investigators. Some of these special relaxation tests will be described in the sequence.

Arulanandan et al. (1971) carried out triaxial tests on specimens of the San Francisco Bay Mud, in which, after the consolidation phase, the drainage was closed and the pore-pressures were measured through time. What was observed was that the pore-

pressure increased with time. They also observed that the longer the soil was allowed to undergo secondary consolidation the lower was the generation of pore-pressure. They reported that similar observations were made by Bjerrum et al. (1958), Campanella (1965) and Walker (1969). Although Walker (1969) has attributed the effect to the arresting of secondary consolidation, Bjerrum et al. (1958) attributed the effect to the diffusion of water through the membrane. Holzer et al. (1973) also observed the same pore-pressure generation pattern as Arulunandan et al (1971) and also ascribed the generation to the arresting of secondary consolidation. Thomasi (2000) and Dos Santos (2006) also observed that same pore-pressure pattern.

As volumetric strains were not allowed and the pore-pressure increased with time, these tests can be considered as relaxation tests under hydrostatic conditions as the mean effective normal stress decreases in time under constant strain and temperature conditions.

Stress relaxation tests carried out in a Constant Rate of Strain edometer apparatus on Sarapui River clay specimens by Lima (1993) showed similar results as those carried out by Arulanandan et al. (1971).

Garcia (1996) carried out drained stress relaxation tests on an organic clay from Barra da Tijuca, Rio de Janeiro. These tests were carried out preventing the specimens from undergoing secondary consolidation by means of load cells/proving rings attached to the edometer apparatus. After the "end" of primary consolidation, the load cell/proving ring was positioned in such a way to prevent the loading arm to move freely, imposing a stress relaxation in the edometer under drained conditions. The Figure below shows the apparatus.

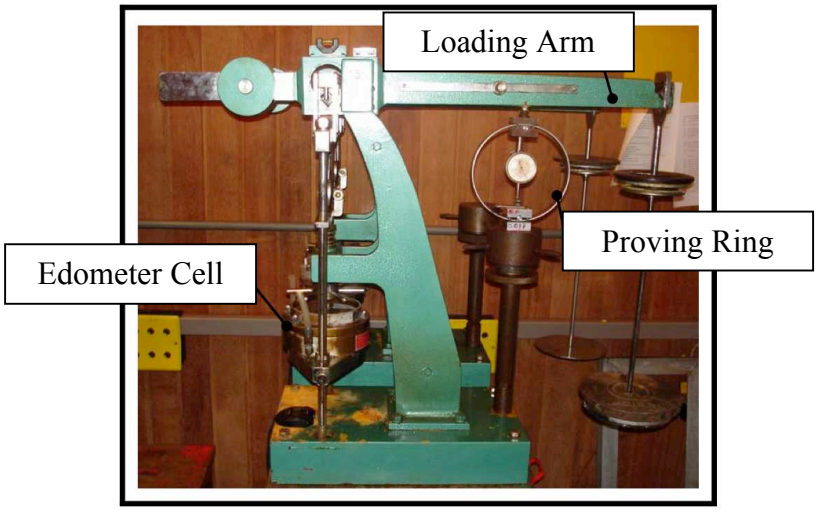

Figure 1 – Apparatus for the execution of relaxation tests in the edometer (modified from Aguiar, 2008).

The tests carried out by Garcia (1996) lasted from about 10,000 to 80,000 minutes. A typical result is shown in the figure below.

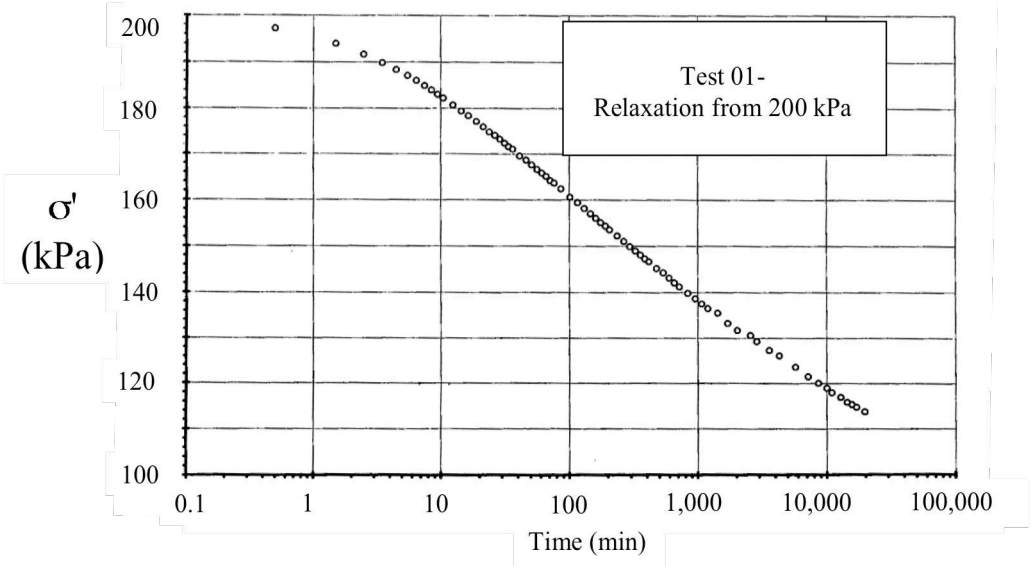

Figure 2 – Typical Result of drained stress relaxation test in the edometer from Garcia (1996).

As it can be seen above, the stress x time (log scale) plot is similar in shape to the tests carried out in the triaxial apparatus, although it can be seen that a very smooth concave curve appears at the latter portion of the plot.

Aguiar (2008) and Andrade (2009) also carried out similar tests as Garcia (1996) and obtained similar results although for a clay from Santos, in the state of São Paulo, Brazil.

Regarding models for explaining time-dependent behavior, one of the main models is the Rate Process Theory. This theory was developed in the area of knowledge called physical chemistry and was originally intended for assessing the speed with which chemical reactions occur. Various investigators such as Murayama and Shibata (1958), Mitchell (1964), Anderson and Douglas (1970) and others applied the Rate Process Theory to soil creep with success. Of particular interest is the work of Lacerda and Houston (1973) where the rate process theory is applied to the stress relaxation problem. Because of its complexity it will not be presented herein. For the fundamentals of the theory it is recommended the study of Glasstone et al. (1940) as well as Mitchell (1964).

Other models intended for explaining time-dependent behavior include visco-elastic, visco-plastic or visco-elasto-plastic models combined or not to the Rate Process Theory or making use of the $c_{\alpha\varepsilon}$ concept. Some of the models in this category are described in Murayama and Shibata (1958, 1961, 1964), Mesri et al (1981), Adachi and Okano (1974), Sekigushi (1984) and Kutter and Sathialingam (1992). As it will be seen in the following section the model developed by Martins's (1992) falls into this category.

Some concepts of Martins's Model (1992)

According to Terzaghi (1941), the contact between clay particles would be of two types. Terzaghi called the contact types "solid bonds" and "film bonds". In his view,

both contacts would be able to transmit effective stresses and would result from the adsorbed water layers that surround the clay particles. The “solid bonds” would result from the contact between the adsorbed water layers in the immediate vicinity of the clay particle, which, according to Terzaghi, would be in the solid state. The “film bonds” would result from the contact between adsorbed water layers which would not be in the solid state but which would possess a viscosity higher than of the viscosity of the free water (by free water it should be understood the water that flows out of the pores of soil during seepage or consolidation).

Having this picture in mind, Martins (1992) assumes as a hypothesis that the shear strength of a saturated normally consolidated clay has two components, the frictional resistance and the viscous resistance.

The frictional resistance would develop between Terzaghi's “solid bonds” and it would be a function of the shear strain. The viscous resistance would develop between Terzaghi's “film bonds” and it would be a function of the strain rate. The equation for the shear strength would then be:

$$\tau = \tau_s + \tau_v = \sigma' \cdot tg\phi'_{mob} + \eta(e) \cdot \dot{\varepsilon} \qquad (1)$$

Where:

τ_s is the solid component of the shear stresses;
τ_v is the viscous component of the shear stresses;
σ' is the normal effective stress;
ϕ'_{mob} is the mobilized effective angle of internal friction;
$\eta(e)$ is the coefficient of viscosity of the adsorbed water layer that surrounds the clays particles (a function of void ratio for a normally consolidated clay); and
$\dot{\varepsilon}$ is the strain rate

The normal effective stress, σ', is taken as the difference between the normal total stress, σ, and pore-pressure, u.

Another hypothesis of the model is that the pore-pressure that develops in a shear test would be a function of the shear strain as shown by Lo (1969a, 1969b). In addition, it is assumed in the model that normalization is valid. In other words, both frictional and viscous resistances are proportional to the consolidation pressure, σ'_c, and are functions of the Over Consolidation Ratio (OCR).

Equation (1) is similar to the equation proposed by Taylor (1948), reproduced below:

$$s = \left(\overline{\sigma}_{ff} + p_i\right) \cdot \left[tg\phi + f\left(\frac{\partial \varepsilon_s}{\partial t}\right)\right] \qquad (2)$$

Where:

s is the shearing strength;
$\overline{\sigma}_{ff}$ is the normal effective stress in the failure plane at failure;

p_i is the intrinsic pressure;
ϕ is the friction angle; and
$\frac{\partial \varepsilon_s}{\partial t}$ is the shear strain rate

Martins (1992) used the tests carried out by Lacerda (1976) on the San Francisco Bay Mud to assess the validity of the proposed model. Without going into much detail in this section, Martins (1992) was able to assess the magnitude of the stress decay that occurred in the relaxation tests carried out by Lacerda (1992), showing that there is a stationary value for the stress relaxation and, therefore, that the process has an end.

One of the problems with Martins's model is that the relaxation is supposed to be instantaneous, what does not occur.

Another problem in the model is that, because Equation (1) is written in terms of shear stresses, the hydrostatic relaxation observed by Arulanandan et al. (1971) and others cannot be macroscopically explained.

To overcome this problem it was suggested by Martins that Equation (1) could be generalized for the normal stresses. In this regard, Thomasi (2000) carried out similar tests as Arulanandan et al. (1971), confirming the possibility of generalizing the normal effective stress equations as proposed by Martins. As the tests carried out by Thomasi (2000) were carried out with water as the triaxial chamber fluid, although carried out with 2 latex membranes coated with silicon grease, diffusion of water was suspected in two tests. Dos Santos (2006) repeated the tests carried out by Thomasi (2000) using silicon oil as the triaxial chamber fluid confirming the conclusions made by Thomasi (2000).

The concepts introduced in this section were intended to provide the minimum information for the development of the stress relaxation study, presented in the next section. For a better understanding of this model the reader is referred to Martins (1992), Martins et al. (2001), Santa Maria et el. (2010) and Santa Maria e al. (2012).

Mechanism of the Stress Relaxation Under Edometric Conditions

General Considerations

According to a proposition made by Martins, which is in agreement with the suggestion made by Terzaghi (1941), the generalized Equation (1) for the normal effective stress would be:

$$\sigma' = \sigma'_s + \sigma'_v \tag{3}$$

Where:

σ' is the normal effective stress;
σ'_s is the normal effective stress that develops in the "solid" contacts between particles and it is a function of the void ratio (or strain) and of the Over Consolidation Ratio (OCR); and

σ'_v is the normal effective stress that develops in the "viscous" contacts between particles and it is a function of the void ratio (or volumetric strain), OCR and the strain rate.

Considering Equation (3) and an axial symmetry stress state such as in the one represented in the figure below:

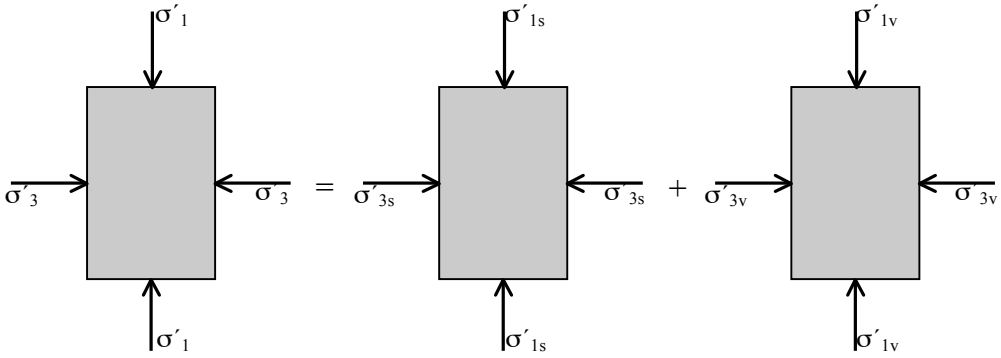

Figure 3 – Stress state under axial symmetry conditions.

It can be shown that the state of stress in the "solid" and "viscous" components of the effective stresses, in addition to Equations (1) and (3) can be represented by the following equations:

$$\sigma'_s = \left(\frac{\sigma'_{1s} + \sigma'_{3s}}{2}\right) + \left(\frac{\sigma'_{1s} - \sigma'_{3s}}{2}\right) \cdot \cos(2 \cdot \alpha) \tag{4}$$

$$\tau_s = \left(\frac{\sigma'_{1s} - \sigma'_{3s}}{2}\right) \cdot sen(2 \cdot \alpha) \tag{5}$$

$$\sigma'_v = \left(\frac{\sigma'_{1v} + \sigma'_{3v}}{2}\right) + \left(\frac{\sigma'_{1v} - \sigma'_{3v}}{2}\right) \cdot \cos(2 \cdot \alpha) \tag{6}$$

$$\tau_v = \left(\frac{\sigma'_{1v} - \sigma'_{3v}}{2}\right) \cdot sen(2 \cdot \alpha) \tag{7}$$

Where the indexes "s" and "v" represent the "solid" and the "viscous" components of the stresses and the indexes "1" and "3" represent the major and minor principle stresses. In the above equations and for a given plane, α is the angle between the direction perpendicular to the plane considered and the plane where σ'_1 acts.

Considering again Equation (3), it can be seen that, for a given strain, the higher the strain rate the greater the viscous stress component and the normal effective stress. This equation is in agreement with experimental data from triaxial and edometric stress. Examples of this experimental observation are the triaxial tests carried out by

Vaid and Campanella (1977) and the edometric tests carried out by Leroueil (1985) as shown below.

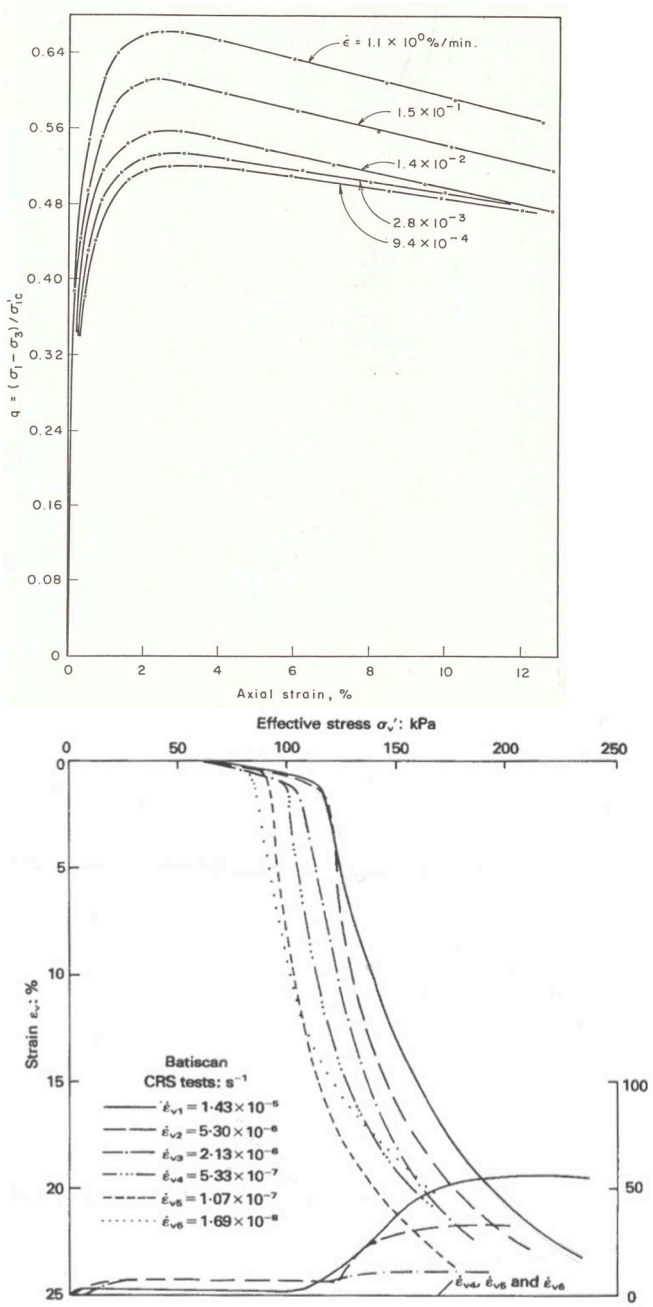

Figures 4 and 5. Examples of the effect of strain rate on triaxial tests (Vaid and Campanella, 1977) and on edometric tests (Leroueil et al., 1985).

As any test is carried out at a given strain rate, according to Equation (3), there will always be an additional resistance to compression. However, if a test could be made with strain rate equal to zero, the only resistance measured would be the resistance from the "solid component" as this component is, by hypothesis, independent of the strain rate.

Limiting the discussion to edometric compression, according to Equation (3), Constant Rate of Strain edometric tests in saturated normally consolidated clay

specimens would present vertical strain x normal effective stress curves such as the ones represented in the figure below.

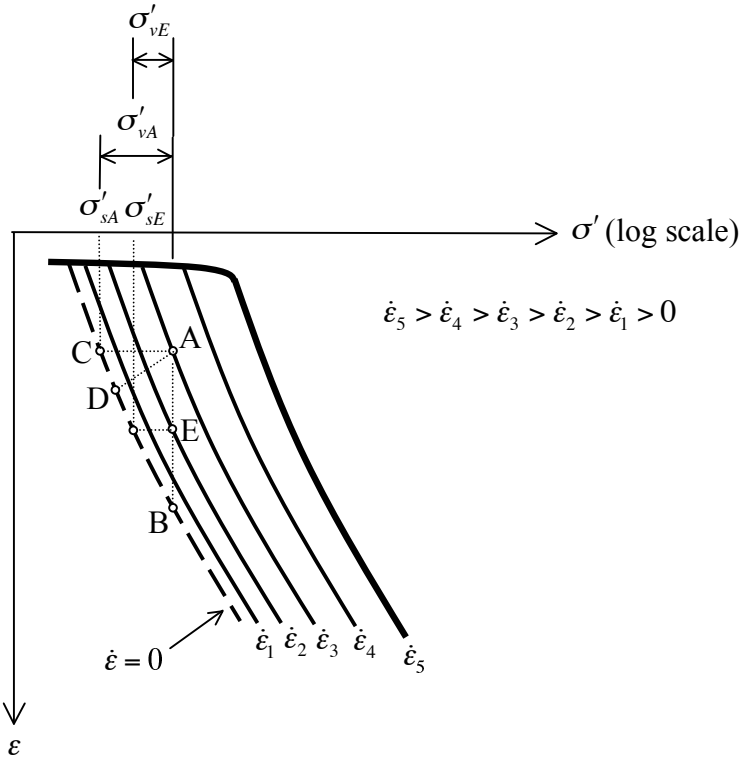

Figure 6 – Schematic representation of Equation (3) for edometric conditions on normally consolidated saturated clay specimens with different strain rates.

As can be seen on Figure 6, the higher the strain rate the greater the normal effective stress for a given strain. Also, according to Figure 6 and Equation (3), for a test with strain rate equal to zero (if such a test could be carried out), there is a unique e x σ' compression curve. The figure above is similar to the one idealized by Taylor (1943) and by Bjerrum (1967). However, the main difference between these figures is that in Figure 6 there is a curve that is independent of rate effects. The curve for which the strain rate is equal to zero was proposed by Martins and represents the end of all rheological processes in his model.

Experimental evidences of the existence of the "zero" strain rate line are provided in Martins (1997), Andrade (2009) and Feijó (1991).

Martins et al. (1997) presents long-term consolidation tests on fabricated clayey soils that lasted between about 2 years showing that secondary consolidation ends and therefore showing that there must be a zero strain rate compression curve such as the one presented on Figure 6.

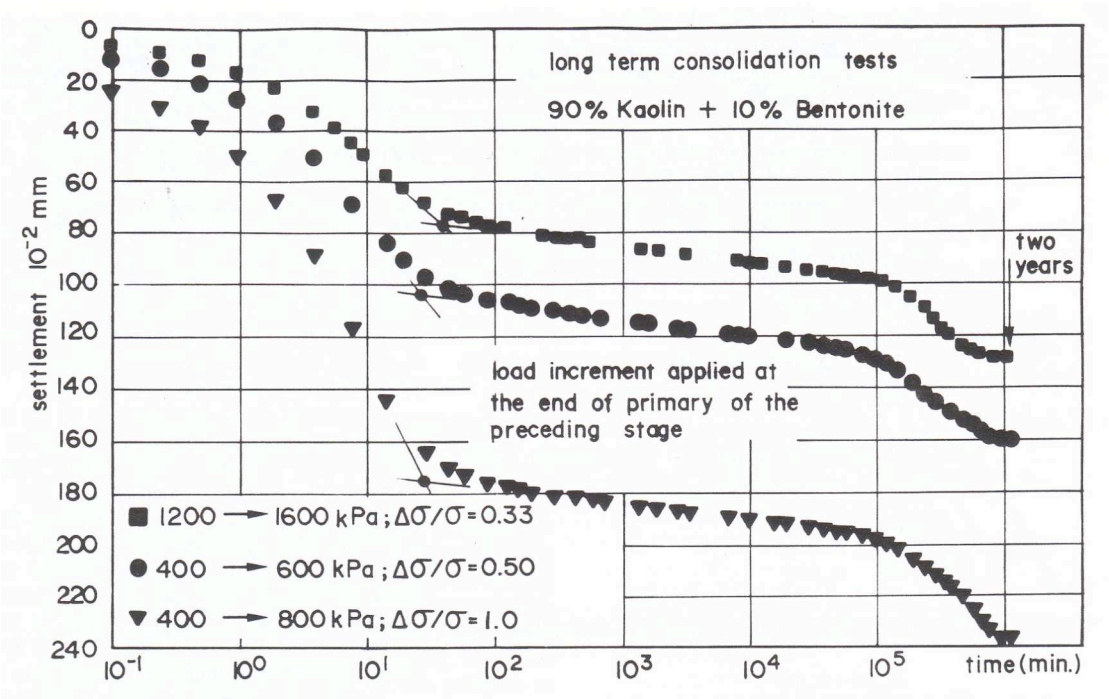

Figure 7 – Long-term consolidation tests carried out by Martins (1997).

Martins carried out long-term consolidation tests that lasted up to 5 years on natural clays from Rio de Janeiro showing that the same reasoning applies also to natural clays. The figure showing the consolidation curve, reproduced from Andrade (2009) is presented below.

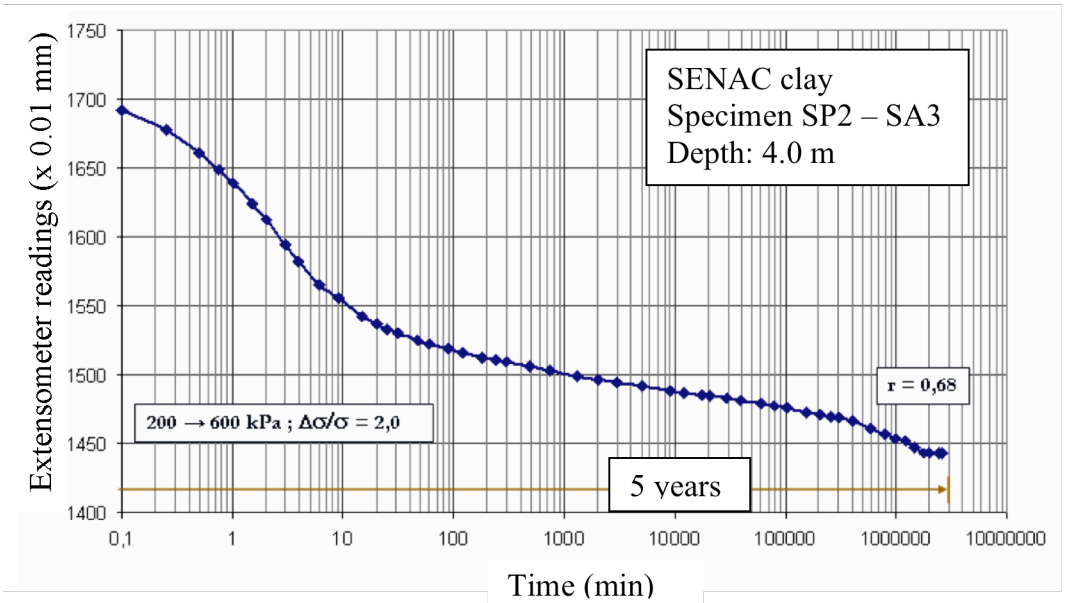

Figure 8 – Long-term consolidation tests carried out by Martins (Apud Andrade, 2009).

The shape of the edometric curves obtained by Martins are in agreement with the shape of the curves of the long term consolidation curves carried out by Bishop and Lovenbury (1969) on the Pancone clay that lasted for about 400 days.

In addition to the long-term consolidation tests, other experimental evidences of the zero strain rate compression curve comes from Feijó (1991), who carried out long-term edometric unload stages with different OCR's on specimens of the Sarapui River clay that lasted up to about 200 days. The results of the tests show that for OCR's less than 2 from the "end" of primary consolidation line, the specimens show a primary expansion following by a recompression. For specimens with OCR's greater than 6, the specimens showed a primary expansion followed by a secondary expansion. For specimens with OCR's between 2 and 6 the specimens showed a primary expansion only, with the expansion ceasing after about 200,000 minutes (approximately 140 days). The void ratio x time curves for the various OCR's generated are shown in the figure below.

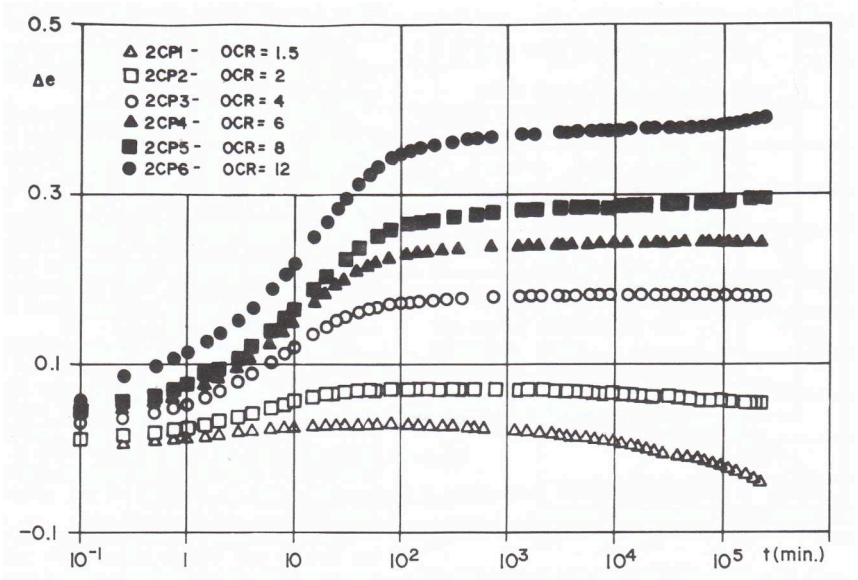

Figure 9 – Test results from Feijo (1991), Apud Martins et al. (1997).

Based on Figure 9 and in the light of the results of the Sarapui River clay, the zero strain rate curve for this clay would be the curve relative to an OCR a little bit higher than 2 from the "end" of primary line.

Now consider a standard consolidation test, where, after the "end" of primary consolidation when the excess pore-pressure is practically zero, a soil specimen is at Point A on Figure 6, where its strain rate is $\dot{\varepsilon}_3$. According to the concepts introduced by Martins, the rheological process represented by segment AB would be secondary consolidation, segment AC represents stress relaxation and segment AD represents a "mixed" condition between secondary consolidation and stress relaxation. Because the rheological process represented by segment AD involves some deformation during the process it can be seen as an "imperfect" stress relaxation.

Similar curves as the ones represented in Figure 6 could be established for hydrostatic or triaxial compression where similar secondary consolidation, creep and stress relaxation processes could be also represented.

As it will be shown further ahead regarding edometric compression, secondary consolidation and stress relaxation can be seen as particular cases of the "imperfect"

stress relaxation process. For clarity reasons, the "imperfect" stress relaxation case will be presented after a discussion about the "perfect" stress relaxation and secondary consolidation processes.

Considering the secondary consolidation process represented by segment AB in Figure 6, at Point A, the soil possesses a "solid" effective stress σ'_{sA} and a "viscous" effective stress σ'_{vA}, relative to the curve with strain rate equal to $\dot{\varepsilon}_3$. With the passage of time, the soil experience a compression and is between Point A and Point B. Naming this point as Point E, at this point, the solid and viscous stresses are σ'_{sE} and σ'_{vE}. From the geometry of Figure 6, at Point E, the soil possesses a greater solid stress than at Point A and a smaller solid stress than at Point B. Because of Equation (3), the viscous stress will have the opposite trend. At Point E, the viscous stress will be smaller than at Point A and greater than at Point B, where the strain rate is zero. Because the viscous resistance is assumed to be proportional to the strain rate, at Point E, the strain rate is smaller than at Point A and greater than at Point B, where the strain rate is zero.

Having this process in mind, secondary consolidation as stated before is the process of transference of viscous stresses to solid stresses under constant vertical effective stress and temperature. With the passage of time, the progress of secondary consolidation imposes the increase of strain and the decrease of the strain rate until the curve with strain rate equal to zero is reached. When the soil reaches this line, the process comes to and end.

In opposition to the secondary consolidation process, the "perfect" stress relaxation process, represented by segment AC, is the decrease of vertical stress at constant strain and temperature. According to Equation (3), a specimen of soil at Point A, if prevented from undergoing secondary consolidation, will have to "march" to the left of Point A, towards the zero strain rate curve by reducing the effective stress until Point C is reached. Because of Equation (3), from the moment the specimen is prevented to deform, the strain rate and the viscous resistance have to drop to zero instantaneously. In other words, the "perfect" stress relaxation, in accordance to Martins's model is considered instantaneous. As the proposition made by Alexandre (2006) only describes the state of stress incorporating a normal effective stress component of viscous nature, Martins's model as modified by Alexandre (2006) is also not able to explain the "perfect" stress relaxation process.

The "imperfect" stress relaxation process

According to Figure 6, the "imperfect" stress relaxation case is a "mixed" case in the sense that some deformation occurs during the stress decay.

For deducing the differential equation of the "imperfect" stress relaxation process, the set-up conceived by Garcia will be considered first.

Figure 10 below presents the schematic structural system of the "imperfect" stress relaxation test carried out by Garcia (1996) in the edometric apparatus.

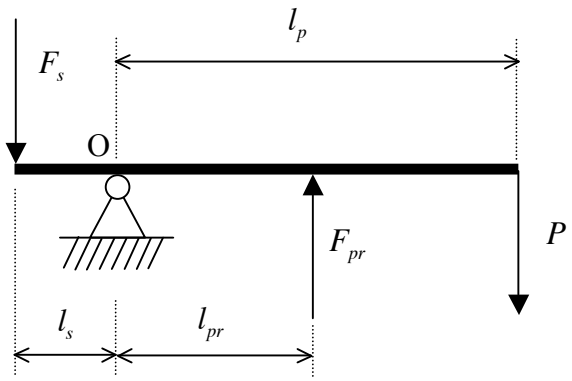

Figure 10 – Schematic structural system of the "imperfect" stress relaxation test as carried out by Garcia (1996).

Considering the shear stresses in the specimen on a plane where its normal makes an angle of 45° with the direction of the major principal effective stress, σ'_1, the following equation can be written:

$$\tau = \left(\frac{\sigma_1 - \sigma_3}{2}\right) = \tau_s + \tau_v = \left(\frac{\sigma'_{1s} - \sigma'_{3s}}{2}\right) + \left(\frac{\sigma'_{1v} - \sigma'_{3v}}{2}\right) \tag{8}$$

The equation above can be obtained by combining equations (1), (5) and (7).

Multiplying Equation (8) by 2 one gets:

$$\left(\sigma_1 - \sigma_3\right) = \left(\sigma'_{1s} - \sigma'_{3s}\right) + \left(\sigma'_{1v} - \sigma'_{3v}\right) \tag{9}$$

Which, by its turn can be re-written as:

$$\left(\sigma_1 - \sigma_3\right) = \left(\sigma'_{1s} + \sigma'_{1v}\right) - \left(\sigma'_{3s} + \sigma'_{3v}\right) \tag{10}$$

Considering that the coefficient of earth pressure at rest, K_0, can be represented by:

$$K_0 = \frac{\sigma'_3}{\sigma'_1} = \frac{\sigma'_{3s} + \sigma'_{3v}}{\sigma'_{1s} + \sigma'_{1v}} \tag{11}$$

The following can be written:

$$\left(\sigma_1 - \sigma_3\right) = \left(\sigma'_{1s} + \sigma'_{1v}\right) - K_0 \cdot \left(\sigma'_{1s} + \sigma'_{1v}\right) \tag{12}$$

Equation (12) can be re-written as:

$$\left(\sigma_1 - \sigma_3\right) = \left(\sigma'_{1s} + \sigma'_{1v}\right) \cdot \left(1 - K_0\right) \tag{13}$$

Considering that at the "end" of primary consolidation, the excess pore-pressure is practically zero, follows that:

$$\sigma \approx \sigma' = \sigma'_s + \sigma'_v \tag{14}$$

In this particular case, K_0 can also be written in terms of total stress, such that:

$$K_0 \approx \frac{\sigma_3}{\sigma_1} \tag{15}$$

Combining Equations (13) and (15) yields:

$$\left(\sigma_1 - K_0 \cdot \sigma_1\right) = \sigma_1 \cdot \left(1 - K_0\right) = \left(\sigma'_{1s} + \sigma'_{1v}\right) \cdot \left(1 - K_0\right) \tag{16}$$

Which can be simplified to become:

$$\sigma_1 = \sigma'_{1s} + \sigma'_{1v} \tag{17}$$

Equation (17) is the nuclei of the differential equation of the "imperfect" stress relaxation process. In other words, the stress relaxation process under edometric conditions consist of a stress decay in σ'_1 only. The complete differential equation is obtained by combining Equation (17) with the functions that describe the solid and the viscous components of the normal effective stress and the function that describes how the total normal stress varies with the rigidity of the system in the edometric apparatus.

For σ'_{1s}, the following can be written at Point A:

$$\sigma'_{1s} = \sigma'_{1sA} + E_{ed} \cdot \varepsilon \tag{18}$$

Where:

σ'_{1sA} is the solid component of the normal effective stress at Point A;
E_{ed} is the edometric modulus for a given stress range at the vicinity of Point A; and
ε is the vertical strain in relation to Point A.

For σ'_{1v}, based on the findings of Martins (1992) and Alexandre (2000, 2006), in a first approximation, the following can be written:

$$\sigma'_{1v} = K \cdot \left(\dot{\varepsilon}\right)^n \tag{19}$$

Where:

K and n are constants to be determined experimentally (being K a function of the void ratio and OCR); and
$\dot{\varepsilon}$ is the strain rate

For discussions about the non-linear viscosity function the reader is referred to Martins (1992), Alexandre (2000), Martins et al (2001), Santa Maria (2010) and Santa Maria (2012).

Therefore Equation (17) can be written as:

$$\sigma_1 = \sigma'_{1sA} + E_{ed} \cdot \varepsilon + K \cdot \left(\dot{\varepsilon}\right)^n \tag{20}$$

Considering Figure (10), considerations of static equilibrium yields the following equation for the total normal stress:

$$\sigma_1(t) = \frac{P \cdot l_p - F_{pr} \cdot l_{pr}}{l_s \cdot A_s} \tag{21}$$

Where:

$\sigma_1(t)$ is the total normal stress as a function of the time t;
P is the dead weight applied at the end of the loading arm of the edometric apparatus;
F_{pr} is the force measured in the proving ring; and;
A_s is the area of the cross section of the specimen of soil to be tested.

For $t = 0$, the force measured at the proving ring is zero and therefore:

$$\sigma_1(0) = \sigma_0 = \frac{P \cdot l_p}{l_s \cdot A_s} \tag{22}$$

Combining Equations (20) and (21) follows that:

$$\sigma_1(t) = \frac{P \cdot l_p - F_{pr} \cdot l_{pr}}{l_s \cdot A_s} = \sigma'_{1sA} + E_{ed} \cdot \varepsilon + K \cdot \left(\dot{\varepsilon}\right)^n \tag{23}$$

Assuming that for small displacements and strains the load measured on the proving ring is proportional to the vertical displacements on the proving ring, one may write the following:

$$F_{pr} = k \cdot x \tag{24}$$

Where:
k is the constant of the proving ring;
x is the displacement experienced by the proving ring as a result of a force F_{pr} acting on it.

Considering also that the vertical strain and vertical strain rate can be written as:

$$\varepsilon = \frac{x_s}{H_s} \text{ and } \dot{\varepsilon} = \frac{d}{dt}\left(\frac{x_s}{H_s}\right) = \frac{1}{H_s} \cdot \left(\frac{dx_s}{dt}\right) \tag{25) and (26}$$

Where:

x_s is the vertical displacement of the top surface of soil specimen in relation to the bottom surface;
H_s is the height of soil specimen at the beginning of the stress relaxation test; and
t is time since the beginning of the stress relaxation.

The following can be written:

$$\frac{P \cdot l_p - k \cdot x \cdot l_{pr}}{l_s \cdot A_s} = \sigma'_{1sA} + E_{ed} \cdot \left(\frac{x_s}{H_s}\right) + K \cdot \left(\frac{1}{H_s} \cdot \frac{dx_s}{dt}\right)^n \tag{27}$$

From the geometry of the "imperfect" stress relaxation test (Figure 10), assuming a rotation of the loading arm as a rigid body, follows that x and x_s are related by the following equation:

$$x = \frac{l_{pr}}{l_s} \cdot x_s \tag{28}$$

Therefore the differential equation of the "imperfect" stress relaxation process under edometric conditions is:

$$\frac{P \cdot l_p - k \cdot \left(l_{pr}^2 / l_s\right) \cdot x_s}{l_s \cdot A_s} = \sigma'_{1sA} + E_{ed} \cdot \left(\frac{x_s}{H_s}\right) + K \cdot \left(\frac{1}{H_s} \cdot \frac{dx_s}{dt}\right)^n \tag{29}$$

Equation (29) is similar to the differential equation of the undrained creep in the triaxial apparatus as obtained by Alexandre (2006).

For brevity, the mathematical deduction of the solution of Equation (29) will be omitted and the solution will be presented below:

For $t = 0$, at the beginning of the "imperfect" stress relaxation process follows that $x_s = 0,\ F_{pr} = 0$ e $\frac{dx_s}{dt} = H_s \cdot \left[\frac{\left(\frac{P \cdot l_p}{l_s \cdot A_s}\right) - \sigma'_{1sA}}{K}\right]^{\frac{1}{n}}$ and therefore the solution to Equation (29) for these initial conditions is:

$$x_s(t) = \left(\frac{A}{B'}\right) - \left(\frac{D}{B'}\right) \cdot \frac{1}{\left[\left(\frac{D}{A}\right)^{\left(\frac{1-n}{n}\right)} + \left(\frac{1-n}{n}\right)\frac{B' \cdot t}{D}\right]^{\left(\frac{n}{1-n}\right)}} \tag{30}$$

Where t is the time since the beginning of the stress relaxation process and A, B, C, B' and D are auxiliary variables defined as below:

$$A = \frac{P \cdot l_p}{l_s \cdot A_s} - \sigma'_{1sA} = \sigma_1 - \sigma'_{1sA} = \sigma'_{vA},\ B = \frac{k \cdot \left(l_{pr}/l_s\right)^2}{A_s},\ C = \frac{E_{ed}}{H_s},\ B' = \left(C + B\right) \text{ and}$$

$$D = K \cdot \left(\frac{1}{H_s}\right)^n$$

As it will be shown later, an expression of interest is the expression of the rate of displacement of the soil specimen as a function of time as given below:

$$\dot{x}_s = \frac{1}{\left[\left(\frac{D}{A}\right)^{\left(\frac{1-n}{n}\right)} + \left(\frac{1-n}{n}\right)\cdot\frac{B'\cdot t}{D}\right]^{\left(\frac{1}{1-n}\right)}} \tag{31}$$

Considering the equation below:

$$\sigma'(t) = \sigma'_s + \sigma'_v = \sigma'_{1sA} + E_{ed}\cdot\varepsilon + K\dot{\varepsilon}^n = \sigma'_{1sA} + E_{ed}\cdot\left(\frac{x_s}{H_s}\right) + K\cdot\left(\frac{1}{H_s}\cdot\frac{dx_s}{dt}\right)^n \tag{32}$$

The expression of the normal effective stress decay with time is given by:

$$\sigma'(t) = \sigma'_{1sA} + C\cdot\left\{\left(\frac{A}{B'}\right) - \left(\frac{D}{B'}\right)\cdot\frac{1}{\left[\left(\frac{D}{A}\right)^{\left(\frac{1-n}{n}\right)} + \left(\frac{1-n}{n}\right)\frac{B'\cdot t}{D}\right]^{\left(\frac{n}{1-n}\right)}}\right\} + D\cdot\left\{\frac{1}{\left[\left(\frac{D}{A}\right)^{\left(\frac{1-n}{n}\right)} + \left(\frac{1-n}{n}\right)\cdot\frac{B'\cdot t}{D}\right]^{\left(\frac{n}{1-n}\right)}}\right\} \tag{33}$$

The second term to the right of the equal sign in Equation (33) is the gain in the solid component of the effective stress that occurs during the process. The last term to the right of the equal sign in Equation (33) is the stress decay in the viscous component of the effective normal stress.

Substituting $t = 0$ in Equation (33) follows that:

$$\sigma'(0) = \frac{P\cdot l_p}{l_{cp}\cdot A_s} = \sigma_0 \tag{34}$$

Which is the initial stress condition at the beginning of the "imperfect" stress relaxation process and is independent of the rigidity of the system. Evaluating the limit when $t \to \infty$ in Equation (33) follows that:

$$\lim\sigma'(t)_{t\to\infty} = \sigma_{1sA} + \left(\frac{E_{ed}}{H_s}\right)\cdot\frac{\sigma_0 - \sigma'_{1sA}}{\frac{k\cdot\left(l_{pr}/l_s\right)^2}{A_s} + \left(\frac{E_{ed}}{H_s}\right)} \tag{35}$$

A schematic representation of the variation of the solid and viscous components of the normal effective stress as well as the variation of the total normal stress with time is presented in the figure below.

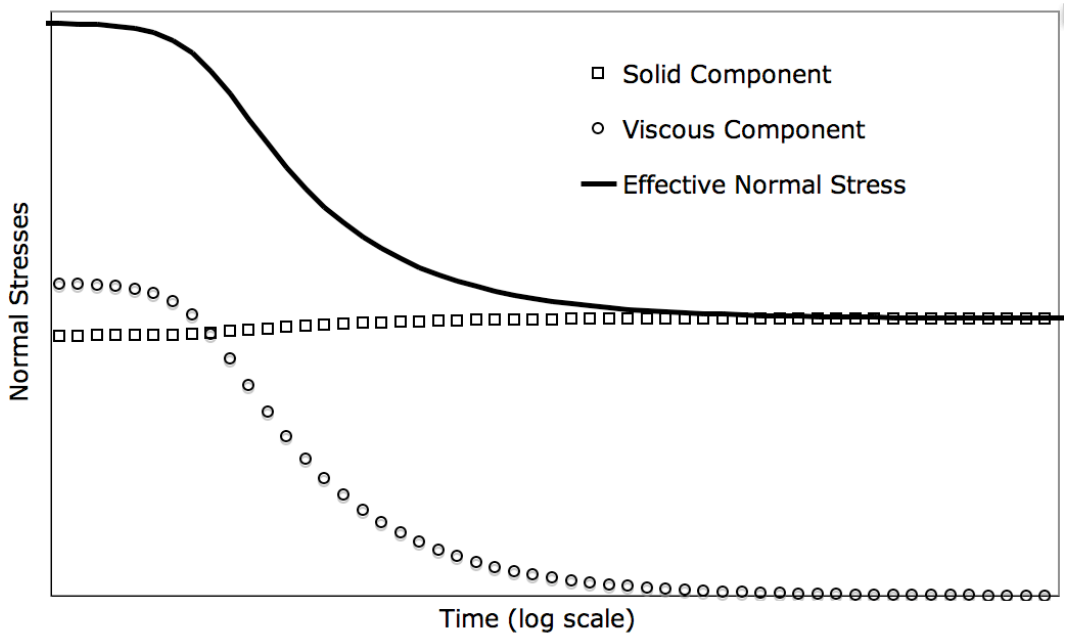

Figure 11 - Schematic representation of the imperfect stress relaxation under edometric conditions.

As shown on Figure 11, the stress decay is due to the decrease of the viscous component in time with only a small portion of the viscous component transferred to the solid component of the effective stress.

The effect of the rigidity of the system can be assessed by making all the other variables constant and varying k on Equation 33. The greater the rigidity the faster the process, which is in accordance to Martins's model. Making $k \to \infty$ on Equation (35) yields $\sigma' = \sigma'_{1sA}$, which is also in accordance to the model.

On the other hand, when making $k \to 0$ the other particular case obtained in the simplified secondary consolidation equation. This equation is simplified because, as the void ratio decrease, the viscosity is expected to increase, and in the derivation of the differential equation it is assumed that the viscosity remains constant through the entire process. Furthermore, the edometric modulus is also considered constant in the derivation of the differential equation. The simplified secondary consolidation process is illustrated in the figure below.

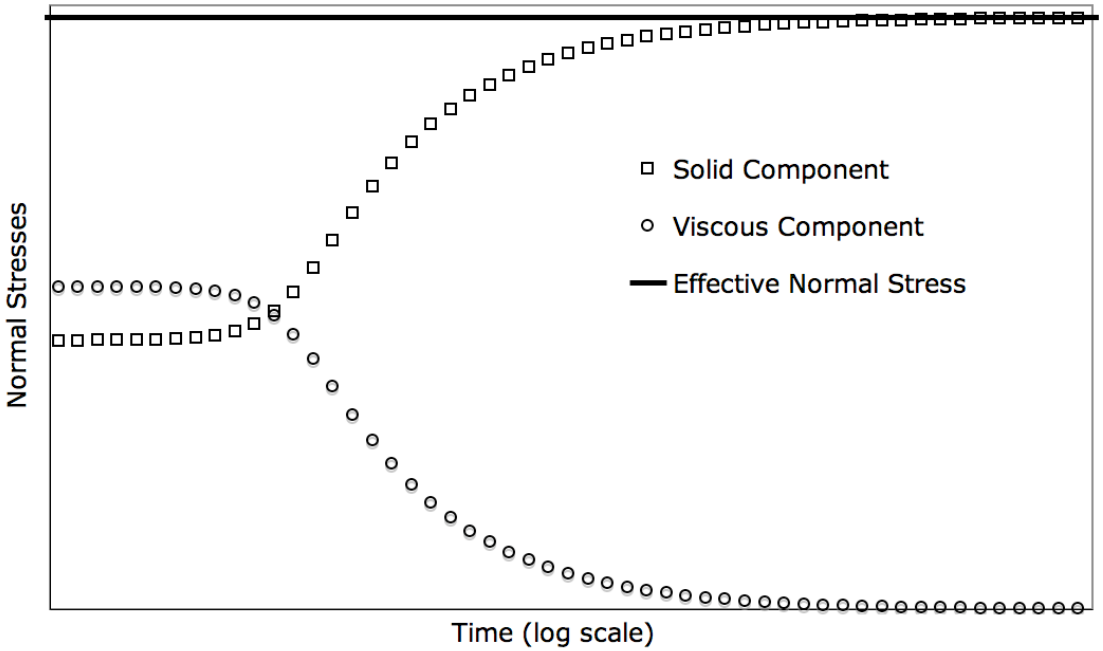

Figure 12 - Schematic representation of the simplified secondary consolidation process under edometric conditions.

When k is made equal to zero on Equation (35) it can be seen that $\sigma'(\infty) = \sigma_0$, which is the particular case of secondary consolidation. This condition is represented by the horizontal solid line on Figure 12. In this particular case, the viscous component of the effective normal stress is entirely transferred to the solid component of the effective stress. This condition is represented by the curves with small circles and small squares on Figure 12, respectively the viscous and solid components.

Beside these differences, the "imperfect" stress relaxation and the secondary consolidation processes have one element in common: the shape of the $\dot{x}_s$ (log scale) x t (log scale) curve, represented by Equation (31).

As can be seen on the figure below, for a constant E_{ed}, the initial portion of the $\dot{x}_s$ (log scale) x t (log scale) curve is convex and the latter portion of the curve is approximately a straight line, which slope is $-1/(1-n)$. The effect of the rigidity, k, on Equation (31) is such that, having all the other parameters the same, the curve is displaced to the left for increasing values of k.

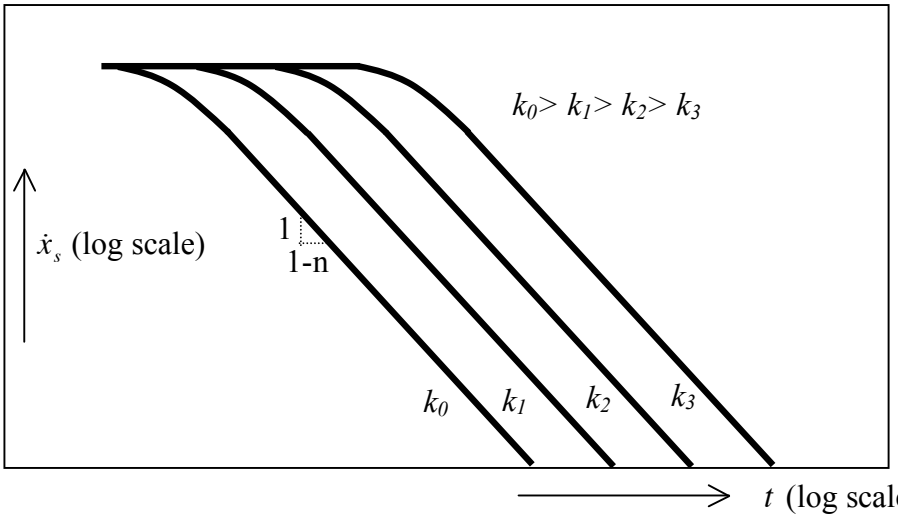

Figure 13 – Shape of the rate of displacement (log scale) x time (log scale) curve.

On the other hand, the effect of the initial viscous component, σ'_v ($\sigma'_v = \sigma_1 - \sigma'_{1sA}$), on Equation (31) is such that, having all the other parameters the same, the curve is displaced in the way showed in the figure below.

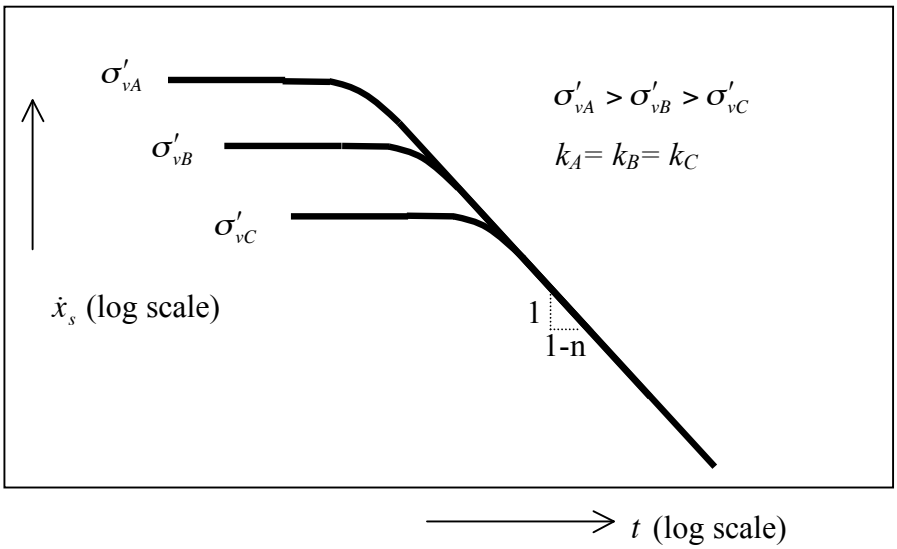

Figure 14 – Shape of the rate of displacement (log scale) x time (log scale) curve for different values of σ'_v and same E.

The reason for having both the creep and the stress relaxation processes the same $\dot{x}_s$ (log scale) x t (log scale) curve shape is that, in the light of the model, the "imperfect" stress relaxation process occurs because of the actual rigidity of the system combined to a creep process. If the "perfect" stress relaxation process were to occur, the stresses would have to decrease instantaneously in the soil as well as in the system. Because the actual rigidity/compressibility of the system, the stress decrease leads to a variation in strain in both the system and in the soil. Therefore, some strain would have to occur in the soil for a zero period of time. In other words, the rate of displacement would be infinite, leading to an infinite viscous resistance, which cannot happen. The instantaneous decrease in stress is prevented by the viscous resistance,

which continues to be mobilized at the beginning of the stress relaxation process. The viscous resistance "holds" the stress decrease, by means of having a strain rate. As time passes both the system and the soil deform, making the system and the "solid" stress to gain part of the viscous component. When this happens, the viscous component decrease by means of a decrease in the strain rate. The process continues until all the viscous component is transferred to system and soil and the strain rate drops to zero at the "zero" strain rate line. The proportion of the viscous component gained by the "solid" component and the system is related to the rigidity of the system and the edometric modulus of the soil. If the system is far more rigid than the soil, a greater proportion of the viscous component goes to the system, otherwise, the soil receives a greater proportion of the viscous component.

Although not easily identifiable, the presence of creep can be seen on Equation (30), which is the solution of the differential equation of the "imperfect" stress relaxation process. A typical plot of the development of displacements in the soil specimen through time in both arithmetic and logarithm scales are presented below.

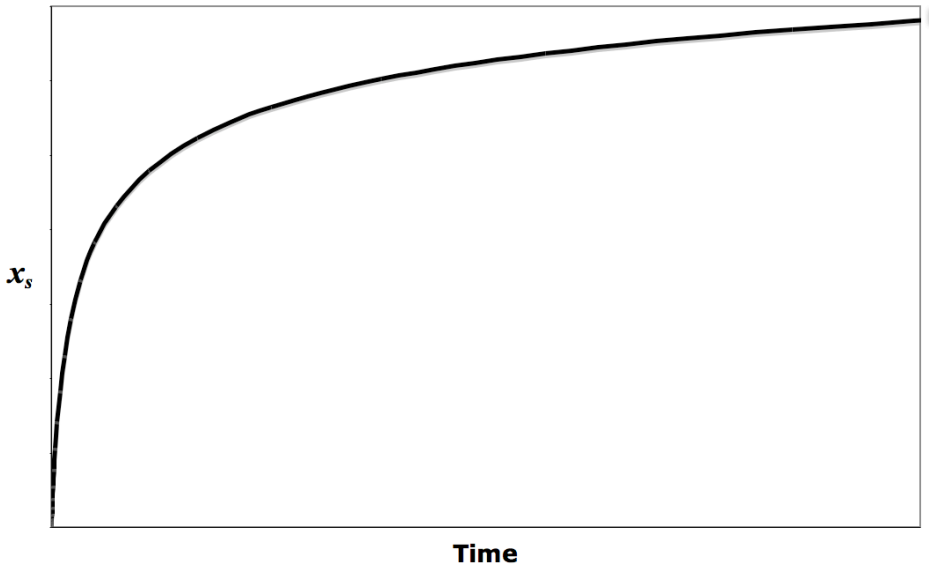

Figure 15 – Strain x time curve – Arithmetic scales.

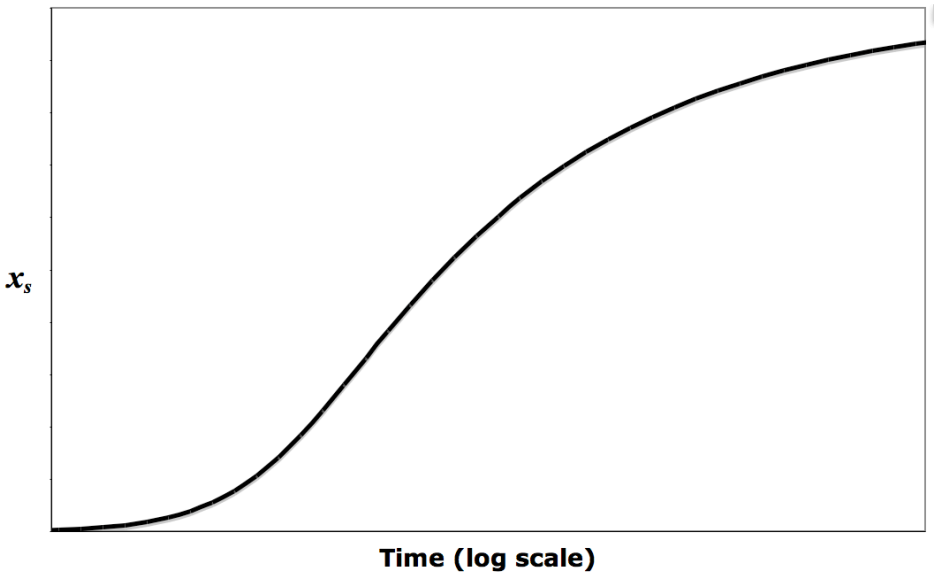

Figure 16 – Strain x time (log scale).

This pattern of deformation resembles the latter portions of the curves of the long-term consolidation tests carried out by Martins (1997), on the latter portions of the curves of the long-term consolidation tests and drained creep triaxial tests carried-out by Bishop and Lovenbury (1969) or on undrained creep triaxial tests carried out by Christensen and Wu (1964).

Finally, it must be said that, because at the "end" of primary consolidation the excess pore-pressure is almost zero, the solution of the differential equation could be represented in terms of total stresses. The solution of the "imperfect" stress relaxation process in terms of total stress can be obtained using the left-hand side of Equation (29) combined to Equation (30).

Predictions

The soil tested

The site where the samples for the testing were taken is located in the Barra da Tijuca area, in Rio de Janeiro, Brazil.

The soil profile at the site consisted of a 3 m layer of peat followed by 10 m of a very soft organic clay, which in turn is underlain by 3 m of compact sand and residual soil. The ground water table was encountered at the ground surface.

The soil tested was a very soft dark grey organic clay containing shell fragments obtained from a depth of 4 m below ground surface using an Osterberg sampler with a length of 900 mm and a diameter of 125 mm. For this soil, Liquidity Limit varied from about 163 % to 314 %, Plastic Limit varied from about 36 % to 140 %, Specific Gravity varied from 2.3 to 2.6 and Natural Water Content varied from about 132 % to 249 %. Pre-consolidation pressure was about 20 kPa.

Regarding the tests carried out by Garcia, the initial conditions were as shown in the table below:

Test Number	Water Content (%)	Total Unit Weight (kN/m^3)	Void Ratio
01	194	12.5	5.05
02	185	12.8	4.75
03	165	12.9	4.29
04	178	12.8	4.59
06	175	13.0	4.44

Table 1 – Initial Conditions of the tests specimens.

All the tests were conducted in a room with temperature control (20±1.5)^o C and water collected from the same borehole as the sample was used in the tests in order to avoid problems related to the chemistry of the water and the adsorbed double layer. Saturation degree was essentially 100 % for all test specimens.

Assessment of the parameters of the model

The figure below shows the lines of equal strain rates obtained by Garcia (1996) from the data of the stress relaxation and secondary consolidation tests carried out by him as well as the assessed zero strain rate line.

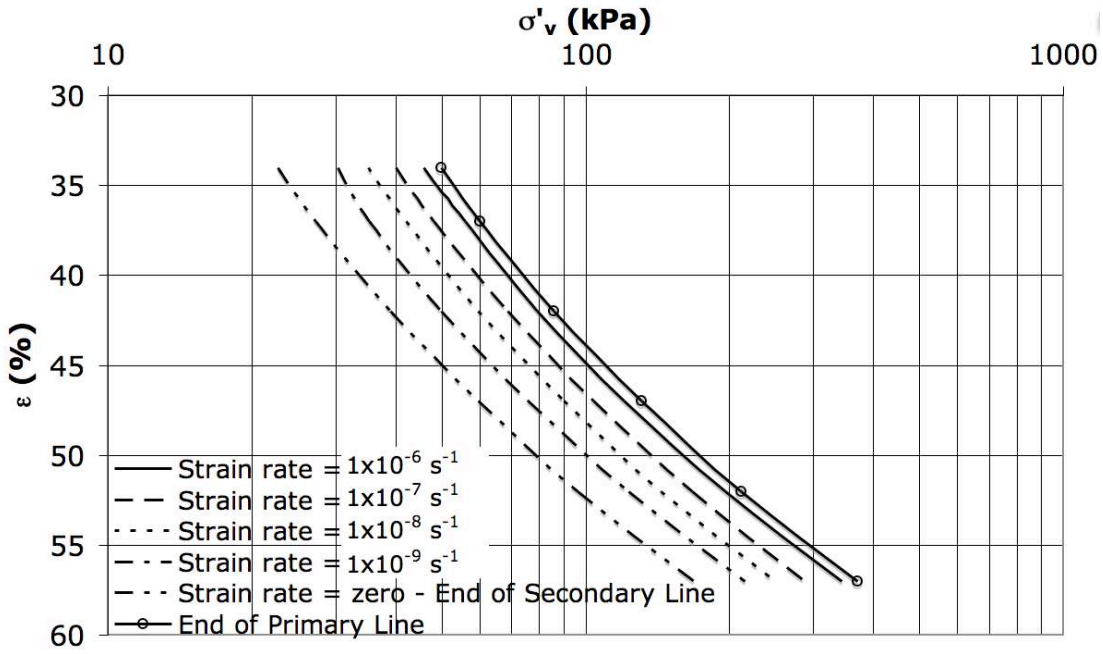

Figure 17 – Lines of equal strain rates for the Barra da Tijuca clay.

Based on Martins's experience on the Sarapui River clay, the "end" of secondary consolidation line can be considered to lay approximately at an OCR of about 2.2 from the "end" of primary line. This line is also presented on Figure 17.

Once assessed the zero strain rate line, the initial solid normal effective stress, σ'_{1s}, and its respective edometric modulus, E_{ed}, can be assessed for each stress relaxation test. Table 2 below presents these values.

Test	Relaxation Stage (kPa)	$\sigma'_{1s}(kPa)$	$E_{ed}(kPa)$
01	50	22.7	114.3
02	50		
03	50		
04	50		
01	100	45.5	378
04	100		
01	200	90.9	965
04	200		
01	400	181.8	1626

Table 2 – Assessed σ'_{1s} and E_{ed} for each stress relaxation test.

As the zero strain rate line is associated with the solid component of the normal effective stress, the viscous component, for a given strain, can be assessed by subtracting the solid effective stress from the effective stress for a curve with a given strain rate. With the viscous components and their respective strain rates, the viscous component function can be assessed.

This assessment resulted in the following viscous effective stress function for the range of consolidation stresses of the stress relaxation tests.

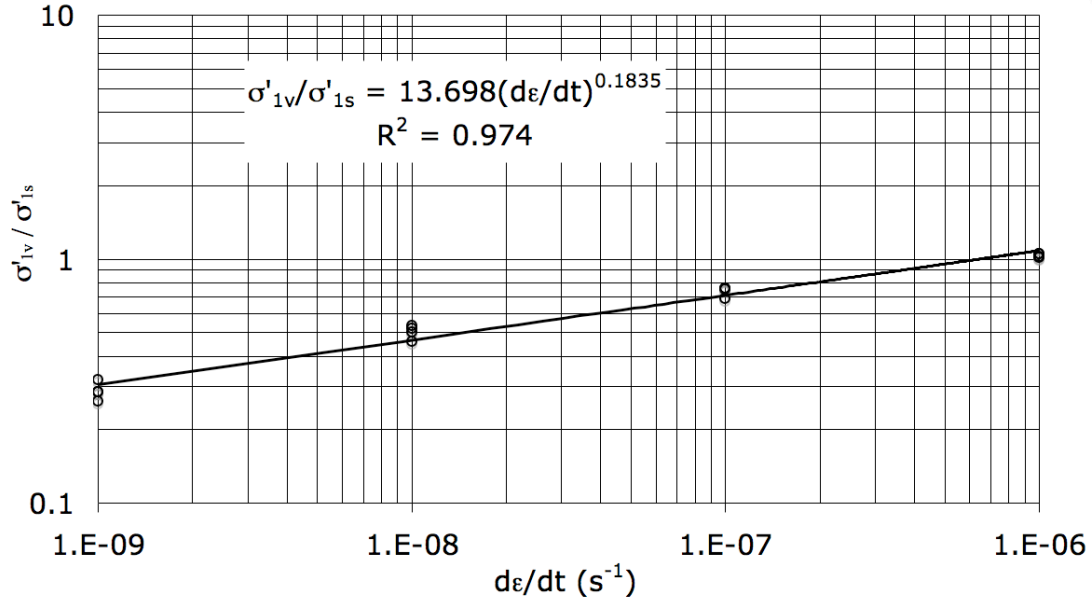

Figure 18 – Assessed viscous function.

For carrying out the predictions of the stress relaxation tests, the only missing component is the rigidity of the system. This can be done based on the figure below.

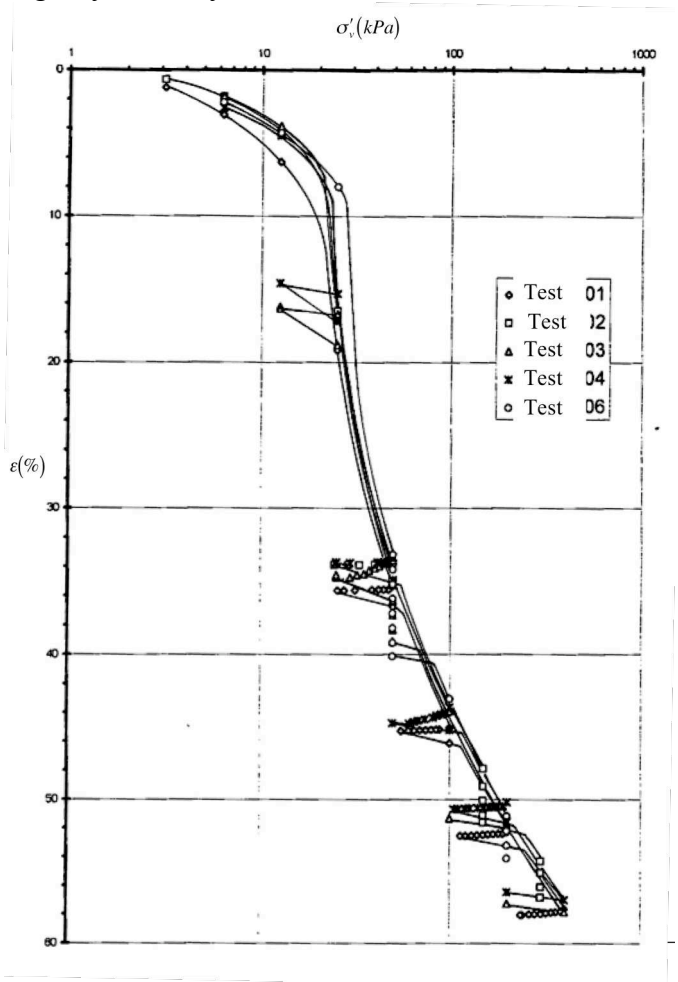

Figure 19 – Compression curve showing the stress relaxation tests.

With the variation in strain and the variation in normal stress experienced at each stress relaxation test and with the dimensions of the consolidation apparatus the equivalent k values were assessed. For the consolidation apparatus used, $l_p = 1.00m$, $l_{pr} = 0.535m, l_s = 0.10m$, $A_s = 0.004m^2$ and $H_s = 20mm$ (initial value of the thicknesses of the samples at the start of the consolidation tests). Table 3 below presents the *k* value for each test.

Test	Relaxation Stage (kPa)	$k(kN/m)$
01	50	72.7
01	100	153.0
01	200	245.5
01	400	417.0
02	50	198.7
03	50	12.6
04	50	50.0
04	100	26.14
04	200	381.9

Table 3 – Assessment of the rigidity of the system.

With the parameters of the model as assessed above, the following predictions were made using Equation (33).

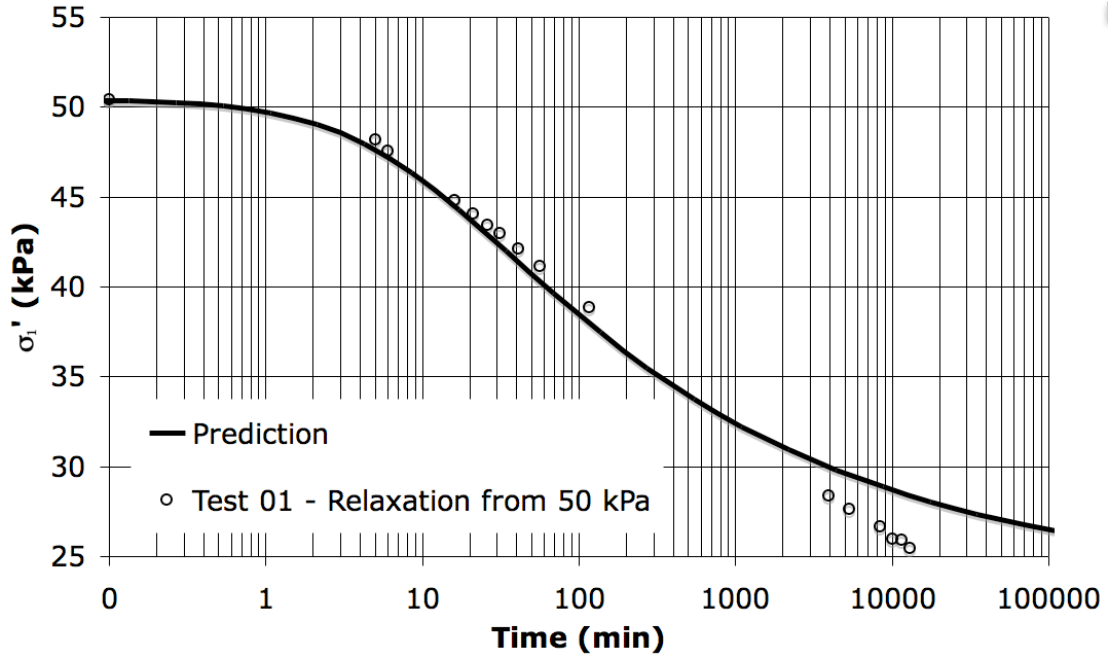

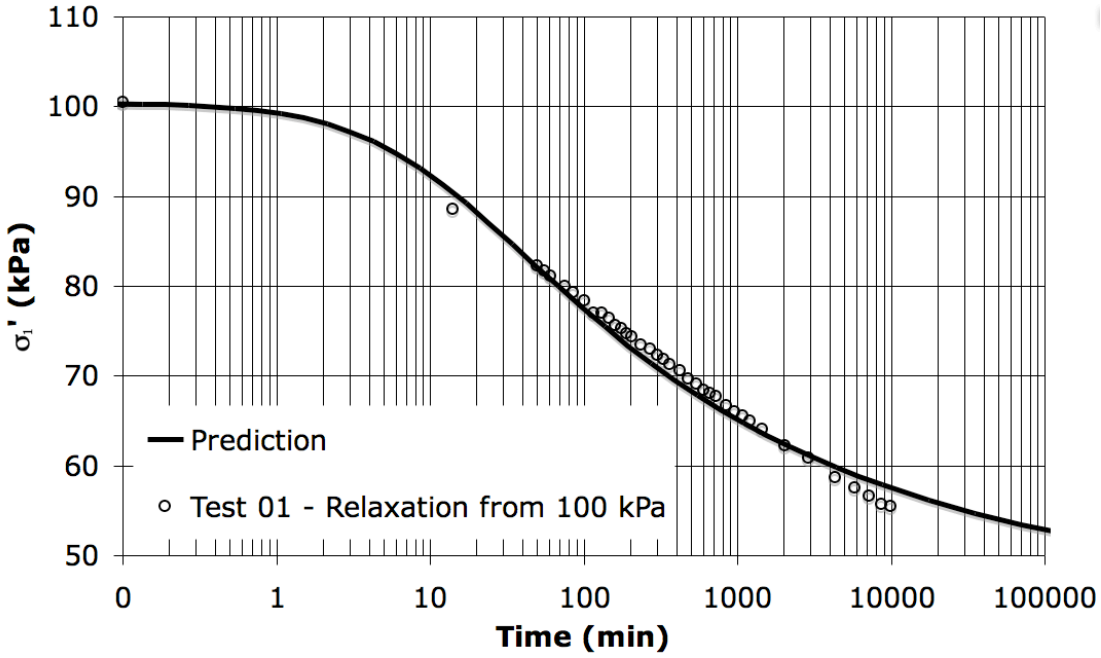
110
100
90
80
70
60
50
σ1' (kPa)
Prediction
Test 01 - Relaxation from 100 kPa
0
1
10
100
1000
10000
100000
Time (min)

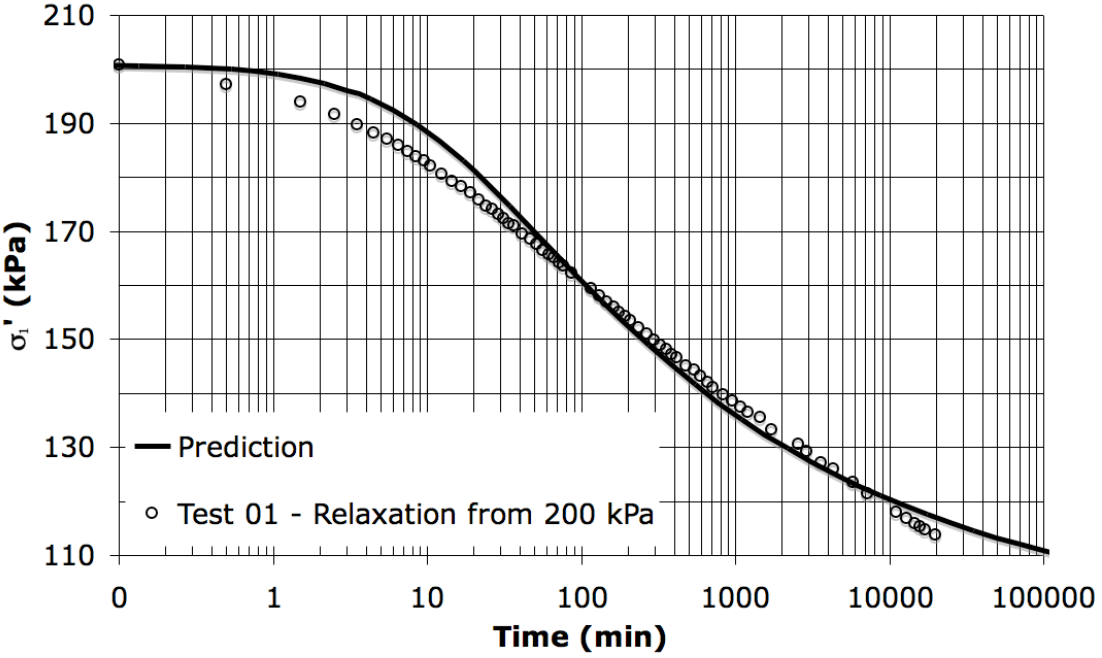
210
190
170
150
130
110
σ1' (kPa)
Prediction
Test 01 - Relaxation from 200 kPa
0
1
10
100
1000
10000
100000
Time (min)

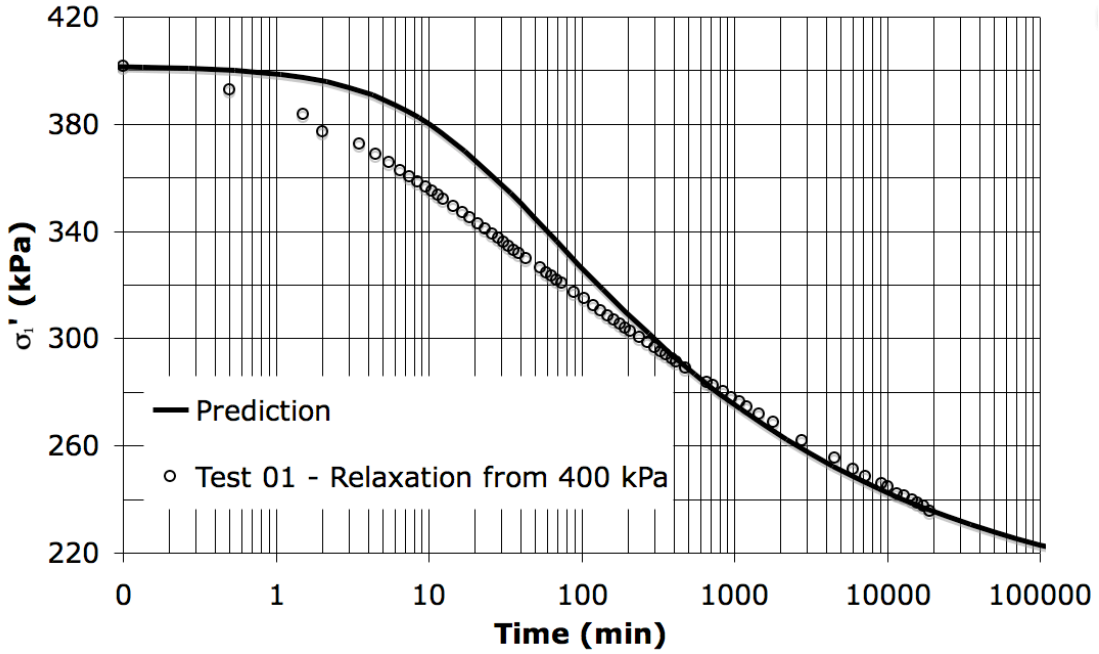
420
380
340
300
260
220
σi' (kPa)
Prediction
Test 01 - Relaxation from 400 kPa
0
1
10
100
1000
10000
100000
Time (min)

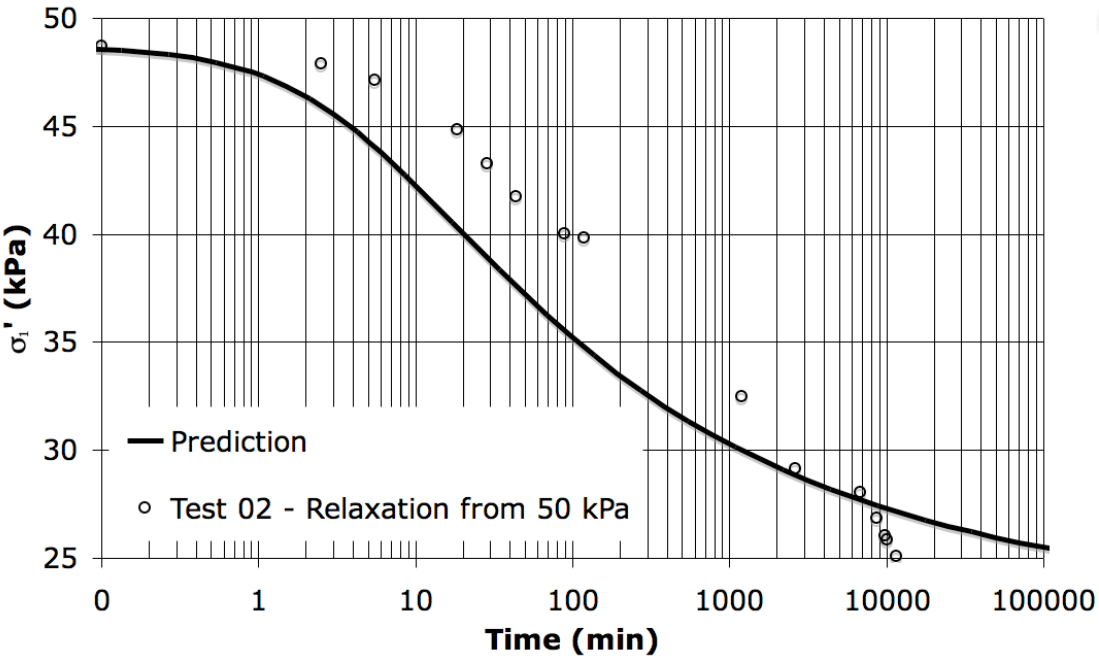
50
45
40
35
30
25
σi' (kPa)
Prediction
Test 02 - Relaxation from 50 kPa
0
1
10
100
1000
10000
100000
Time (min)

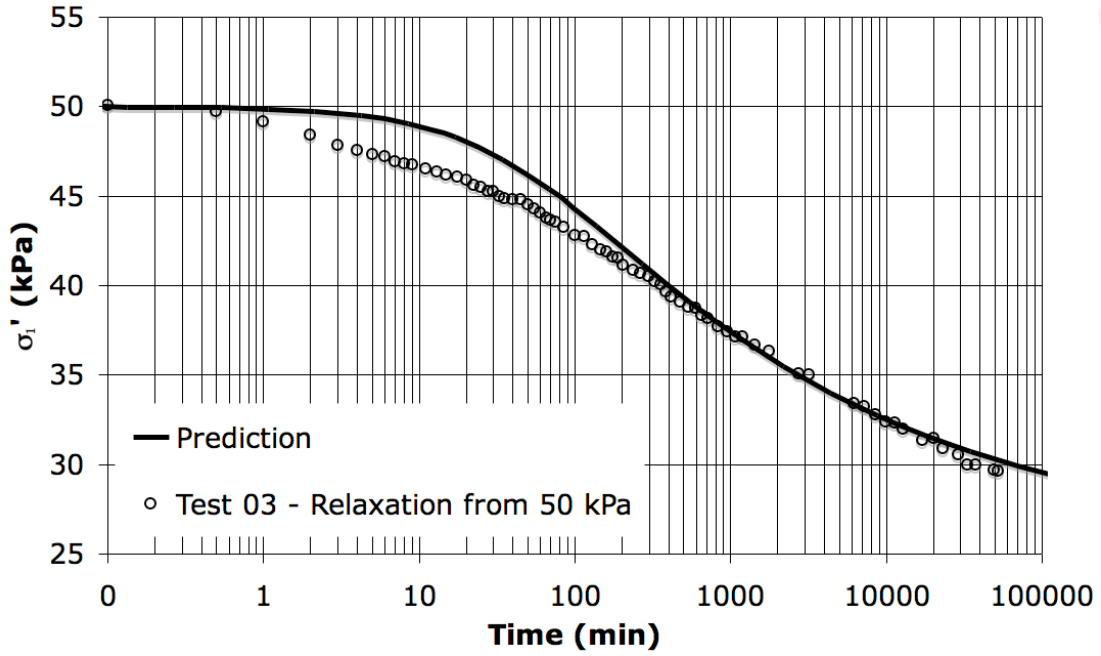
55
50
45
40
35
30
25
σ1' (kPa)
Prediction
Test 03 - Relaxation from 50 kPa
0
1
10
100
1000
10000
100000
Time (min)

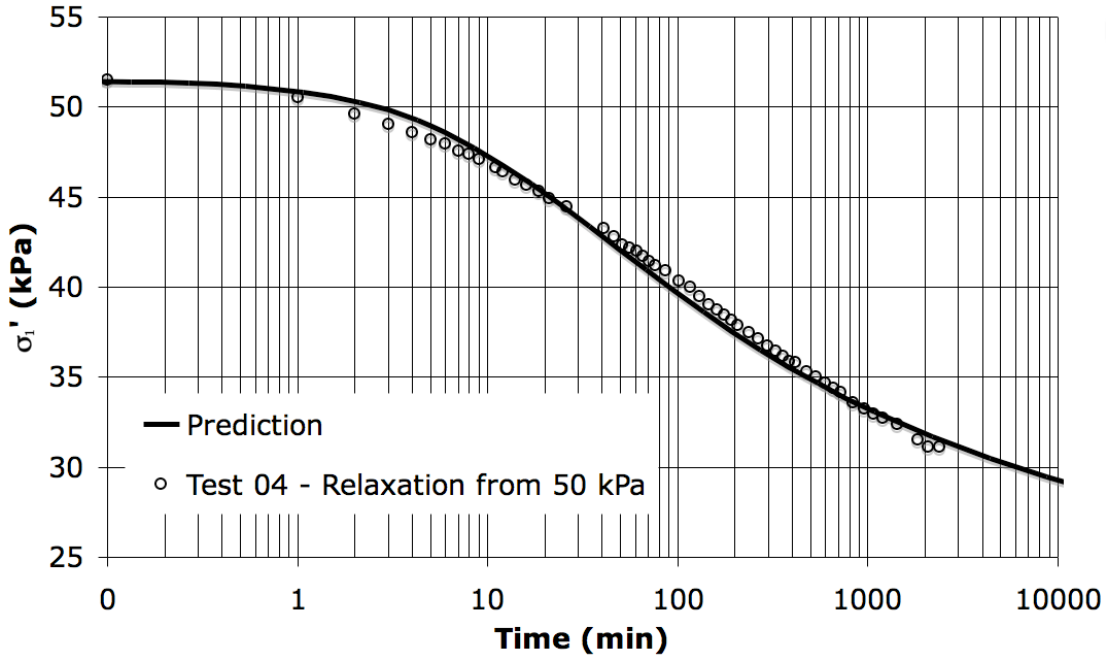
55
50
45
40
35
30
25
σ1' (kPa)
Prediction
Test 04 - Relaxation from 50 kPa
0
1
10
100
1000
10000
Time (min)

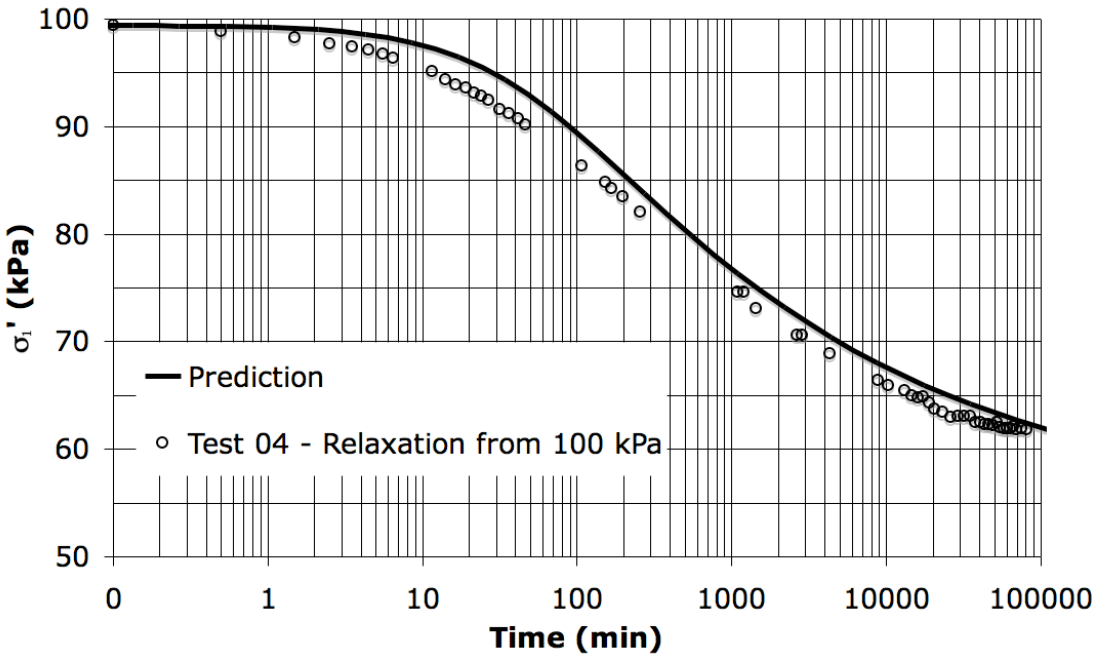

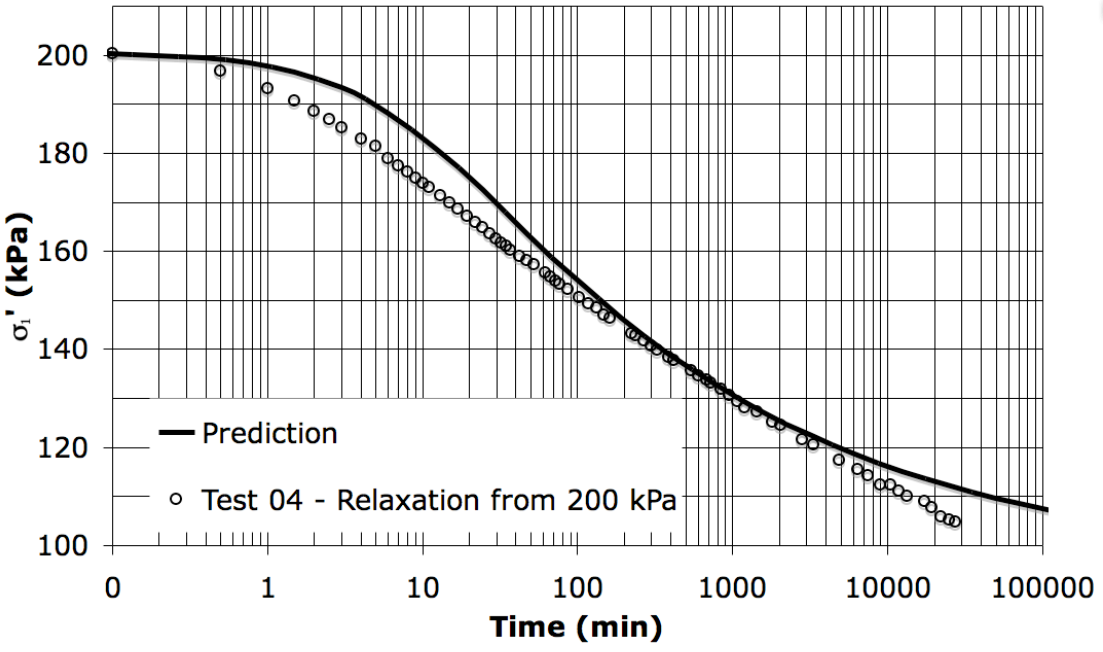

Figure 20 to 28 – Prediction for the relaxation tests carried by Garcia (1996).

Another comparison between predictions and tests results can be made if displacements are measured during stress relaxation. The following plot shows the

comparison between the rate of displacement x time from prediction and from the available tests data from Garcia (1996).

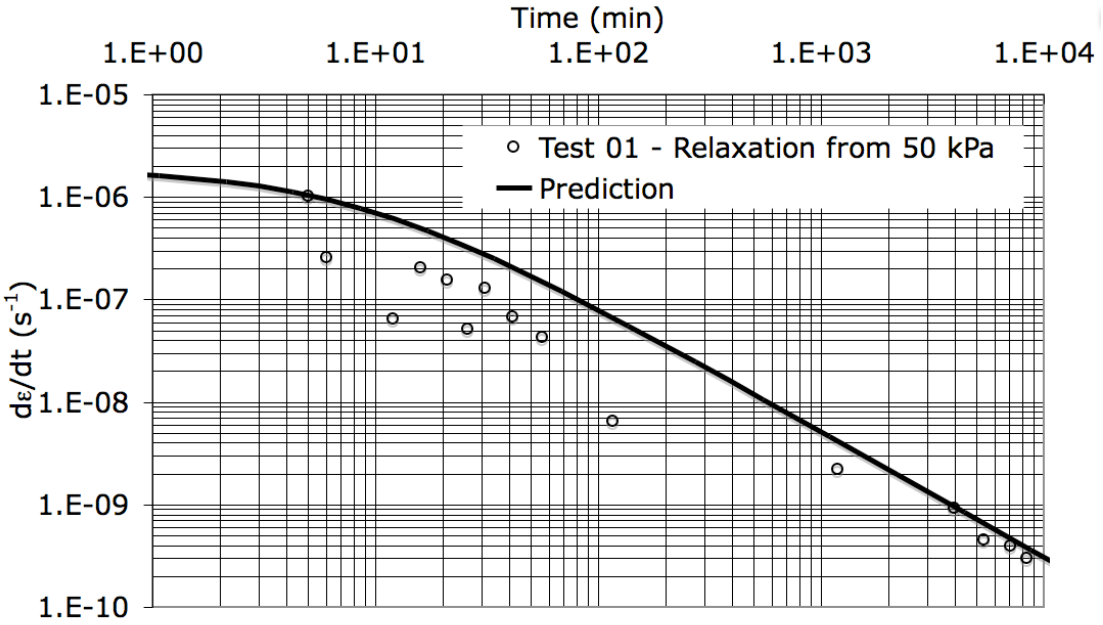

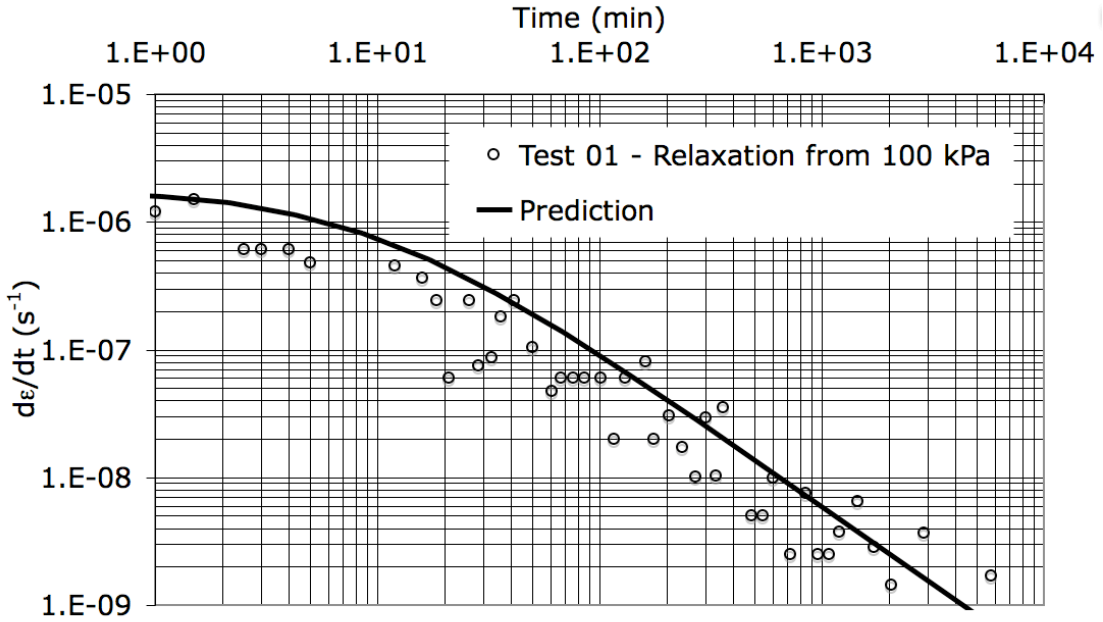

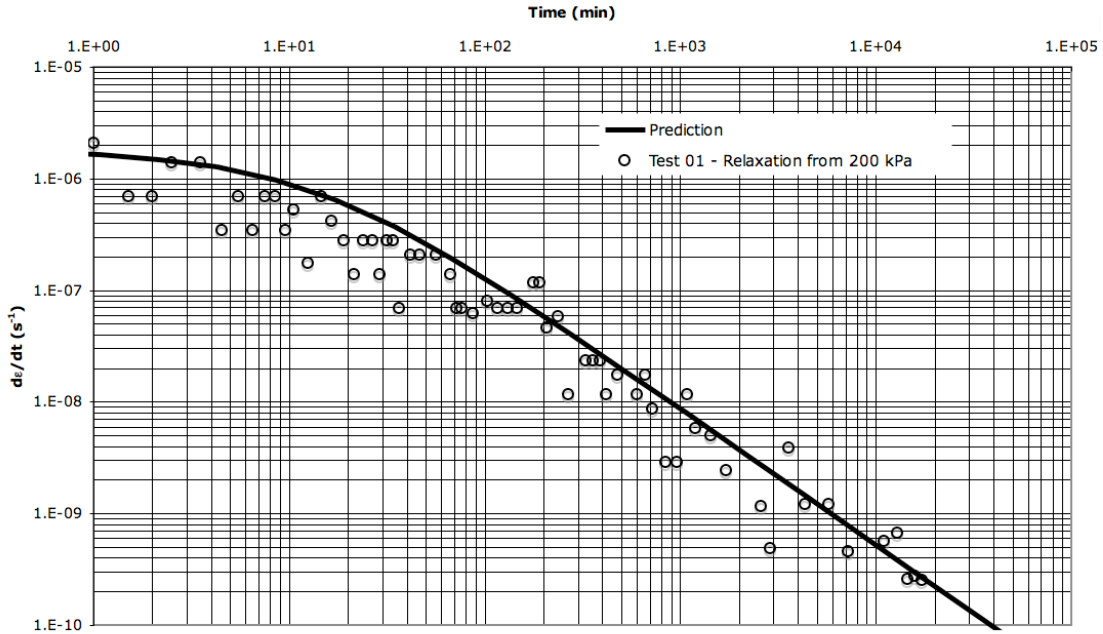
Time (min)
1.E+00
1.E+01
1.E+02
1.E+03
1.E+04
1.E+05
1.E-05
1.E-06
1.E-07
1.E-08
1.E-09
1.E-10
dε/dt (s⁻¹)
Prediction
Test 01 - Relaxation from 200 kPa

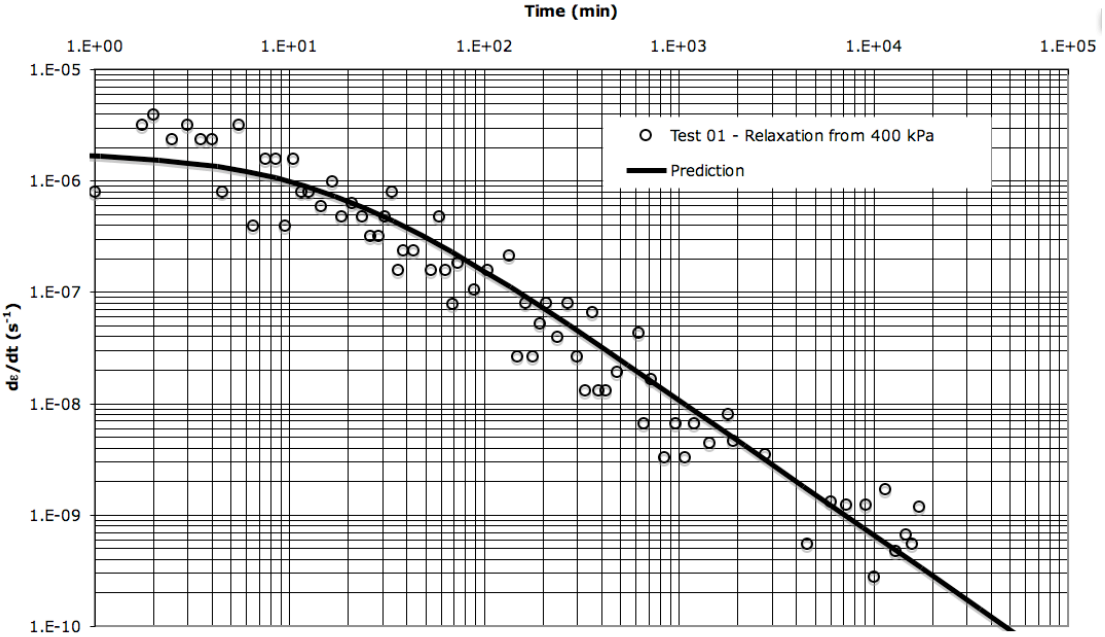
Time (min)
1.E+00
1.E+01
1.E+02
1.E+03
1.E+04
1.E+05
1.E-05
1.E-06
1.E-07
1.E-08
1.E-09
1.E-10
dε/dt (s⁻¹)
Test 01 - Relaxation from 400 kPa
Prediction

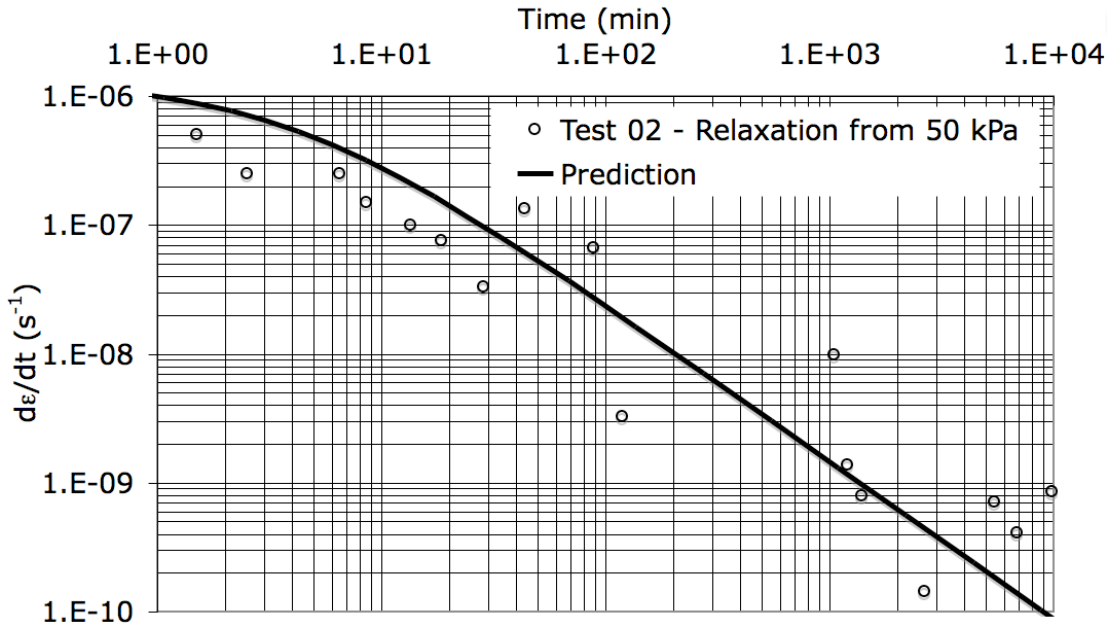
Time (min)
1.E+00
1.E+01
1.E+02
1.E+03
1.E+04
1.E-06
1.E-07
1.E-08
1.E-09
1.E-10
dε/dt (s-1)
Test 02 - Relaxation from 50 kPa
Prediction

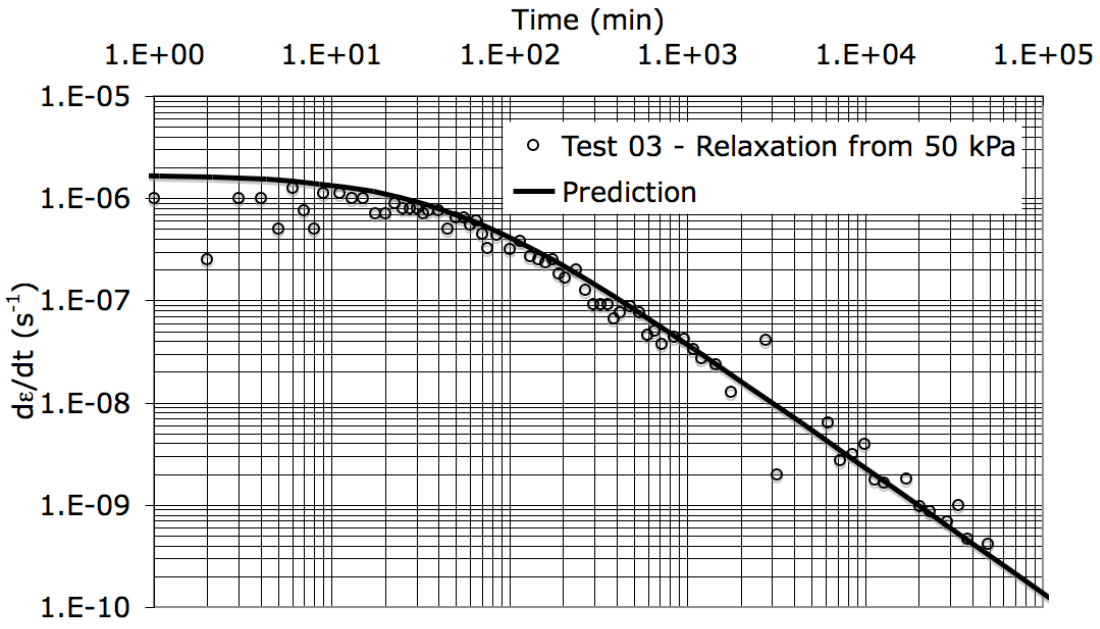
Time (min)
1.E+00
1.E+01
1.E+02
1.E+03
1.E+04
1.E+05
1.E-05
1.E-06
1.E-07
1.E-08
1.E-09
1.E-10
dε/dt (s-1)
Test 03 - Relaxation from 50 kPa
Prediction

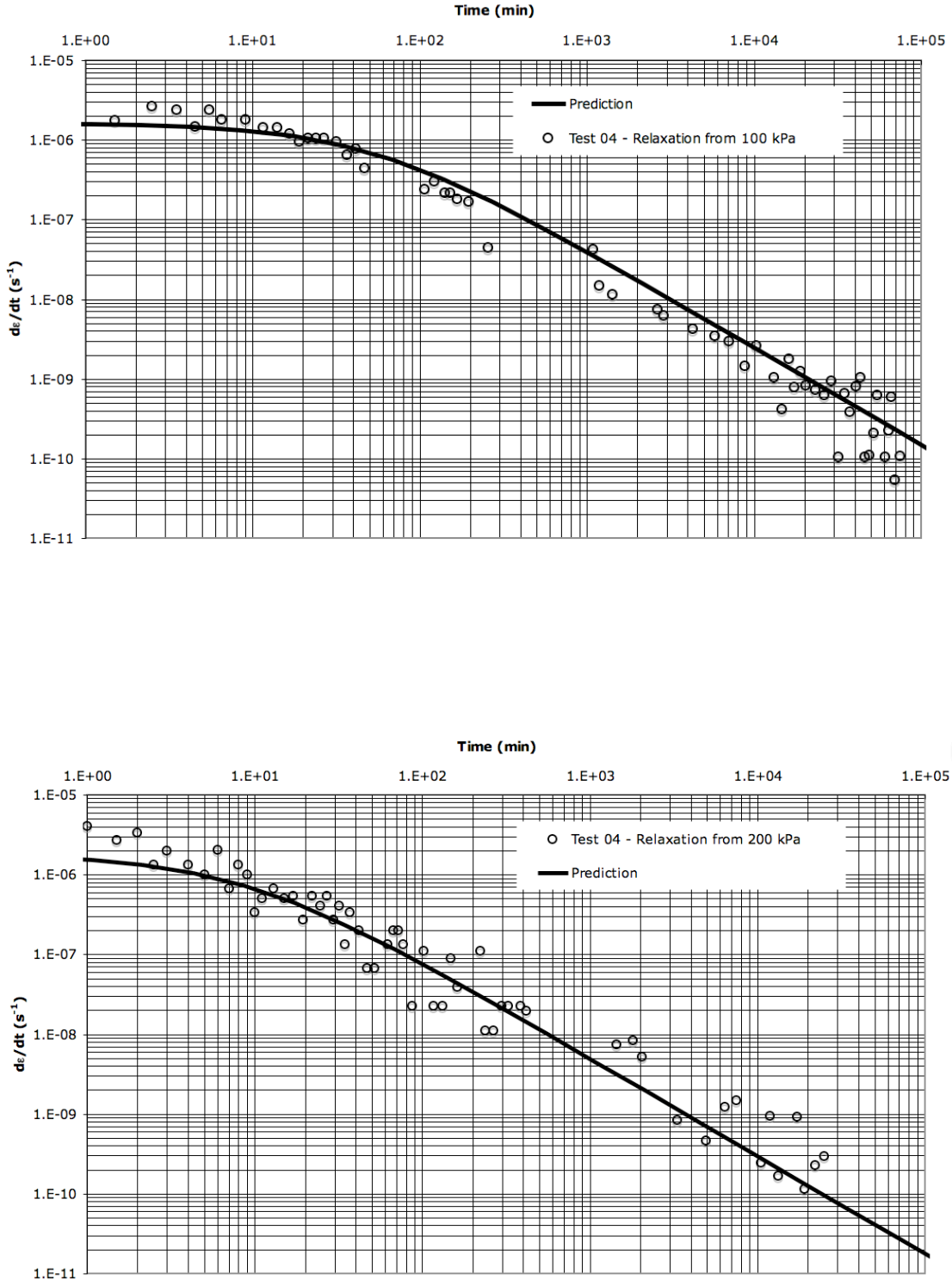

Figure 29 to 35 – Comparison of rate of displacement x time for available data from Garcia (1996).

Discussions

Viscous Component

As can be seen on Figure 18, the power law function adjusts well to the experimental data relative to the viscous components, as the coefficient of correlation demonstrates.

In addition, it can be shown that all the viscous component functions can be normalized as assumed in the model. The normalized viscous component function for this clay is:

$$\sigma'_{1v}/\sigma'_{1s} = 13.698 \cdot \dot{\varepsilon}^{0.1835} \text{ with } R^2 = 0.974 \quad (36)$$

Rigidity of the System

Garcia (1996) mentions the use of load cells and proving rings but he does not indicate which one was used for each test or its characteristics.

Although a more detailed discussion about the rigidity of the system is not possible for the reasons explained above, plots of variation of the force in the load cell/proving ring x displacement of the top surface of the soil specimens show that some accommodation occurs during the stress relaxation. However, the hypothesis of a constant k was found to be reasonable. In addition, as can be seen on Table 2, k varies from test to test. This probably reflects the rigidity of the entire system and not only the rigidity of the load cell or proving ring used.

Predictions of the "Imperfect" Stress Relaxation Tests

As can be seen of Figures 20 to 28, except for the Relaxation Stage from 50 kPa of Test 02, in general, the predictions and tests results are in good agreement both qualitatively and quantitatively.

In addition, as can be seen in Figures 29 to 35 there is good agreement between the rate of displacement x time plots of predictions and tests results.

Although both the predictions and tests results curves present themselves initially convex, becoming concave in the latter part of the curves, the tests results curves are smoother than the prediction curves. The reason for this is unknown, although it is suspected that the discrepancy may be related to the following:

- The viscous component function: The power law function, although it fits the experimental data well, may not be representative for strain rates below $1x10^{-9}$ s^{-1}. In other words, perhaps a better function for representing the viscous component may improve the predictions;
- The rigidity of the system: The variation of the rigidity of the system during the tests (although not very significant) may have an impact on the predictions as it was assumed a constant k for each stress relaxation test;
- The assumption related to the rheological behavior of the model: Equation (20) can be seen to be similar to the equation of a Kelvin-Voigt model, although with a non-linear viscous function. Therefore, the discrepancies may be related to a missing element (i.e. a missing spring or dashpot in series or parallel);
- The assumption regarding σ'_{3v}: As the radial strains are prevented in the edometer, there are no strain rates in the radial direction in macroscopic terms. Therefore, the effective normal stress is assumed equal to σ'_{3s} throughout the entire process. However, in microscopic terms, there may be a σ'_{3v}. If there is

σ'_{3v}, the differential equation obtained may be considered approximate in this regard and a more "exact" equation may be able to provide better predictions.

In face of the reasons mentioned above, more experimental and theoretical research is necessary.

Additional Discussions

The Coefficient of earth pressure at rest, K_0

The last of the reasons for explaining the difference between predictions and tests results is related to the discussion about the variation of the coefficient of earth pressure at rest with time and, as shown by Schmertmann (1983), no definitive answer exists yet for this question.

As per Equation (11), $K_0 = \frac{\sigma'_3}{\sigma'_1} = \frac{\sigma'_{3s} + \sigma'_{3v}}{\sigma'_{1s} + \sigma'_{1v}}$. Therefore, as the viscous component of the normal effective stress vary in time, K_0 is expected to vary in time as well.

In this study, as in macroscopic terms there is no strain rate in the radial direction, it is assumed that $\sigma'_{3v} = 0$. Assuming that there is a K_0 line where the strain rate is equal to zero, just like the zero strain rate compression line, it can be assumed that for this line:

$$K_{0s} = \frac{\sigma'_{3s}}{\sigma'_{1s}} \tag{37}$$

In other words, K_{0s} is independent of time. Equation (11) can be combined to Equation (37) to produce the following equation.

$$K_0 = \frac{K_{0s} \cdot \sigma'_{1s} + 0}{\sigma'_{1s} + \sigma'_{1v}} = \frac{K_{0s} \cdot \sigma'_{1s}}{\sigma'_{1s} + \sigma'_{1v}} \tag{38}$$

Considering stress relaxation first, as σ'_{1s} remains approximately constant throughout the process while σ'_{1v} drops to zero, K_0, according to equation (38) is expected to increase with time to the value $K_0 = K_{0s} = \frac{K_{0s} \cdot \sigma'_{1s}}{\sigma'_{1s}} = \frac{\sigma'_{3s}}{\sigma'_{1s}}$.

On the other hand, during secondary consolidation, $\sigma'_1 = \sigma'_{1s} + \sigma'_{1v} \approx \sigma_1$ remains constant throughout the process as the viscous component is entirely transferred to the solid component. Because σ'_{1s} increases and σ'_{1v} decreases with time while σ'_1 remains constant, the denominator of Equation (38) remains constant while the numerator increases with time. Therefore K_0 increases with time during secondary consolidation as well. The expression for the variation of K_0 with time can be obtained by combining equations (18), (19), (25), (26), (30), (31) and (38).A schematic plot of K_0 with time is presented in the figure below:

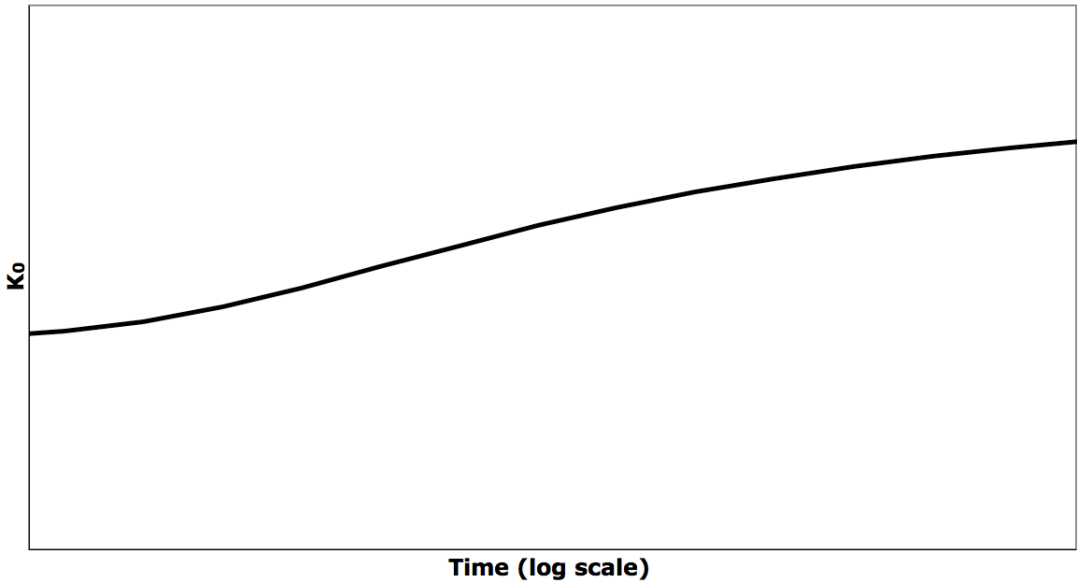

Figure 36 – Schematic representation of the variation of K_0 during secondary consolidation with time according to Equation (38).

As σ'_1 remains constant while $\sigma'_3 = \sigma'_{3s}$ is increasing during secondary consolidation, the shear stresses are relaxing with time, as suggested by Taylor and Merchant (1940).

This trend of increase of K_0 as a consequence of the model appears to be in agreement with the experimental data from Lacerda (1976) and from Kavazanjian and Mitchell (1984).

On the other hand, if a strain rate and a viscous component are considered to exist in microscopic terms in the radial direction it can be shown that K_0 decreases. For this case, considering that the edometric condition could be seen (in a very simplified way) equivalent to a process where first the sample deforms under a drained deviatoric stress condition followed by a radial drained compression that would lead to zero radial strain, K_0 assumes the following equation:

$$K_0 = \frac{\sigma'_3}{\sigma'_1} = \frac{K_{0s} \cdot \sigma'_{1s} + \nu^n \cdot \sigma'_{1v}}{\sigma'_{1s} + \sigma'_{1v}} \tag{39}$$

Where ν is the drained Poisson ratio and n is the exponent of the power function that represents the viscous component of the normal effective stress.

Although a viscous component is considered to exist in microscopic terms in the radial direction, for this case, the differential equation (29) and its solution remain unaltered.

Experimental evidences showing the decrease of K_0 with time also exists (i.e. Santa Maria, 2002).

The results shown in Santa Maria (2002) and well as the ones obtained by Lacerda (1976) and Kavazanjian and Mitchell (1984) may not be confirmed or refuted as some

deformation always occurs in these tests in the radial direction. As the deformation occurs in time, a strain rate and viscous component will always exists, possibly leading to the observations made by the investigators. Although no definite conclusion can be reached at the present it is possible that the model developed by Martins (1992) may have the tools for clarifying this problem.

Although it is not possible to conclude if K_0 will increase or decrease during secondary consolidation, it is possible to show that the solid octahedric effective stresses increase, which is consistent with the decrease in volume that occur during secondary consolidation.

Despite of the problem regarding the possible increase or decrease of K_0, as shown by Equations (38) and (39), it is our opinion that K_0 increases with time during secondary consolidation. For a discussion about these reasons the reader is referred to Lacerda and Martins (1985).

Stress Relaxation Under Triaxial Conditions

In order to explain the mechanics of the stress relaxation in the triaxial apparatus it is first necessary to explain what would happen in CIU test in a saturated normally consolidated clay in agreement with the model developed by Martins (1992).

A Conventional CIU Test in a Normally Consolidated Clay according to Martins's Model

In a CIU test the soil is sheared at a given strain rate with closed drainage (constant void ratio for a saturated clay) after been consolidated to a given consolidation pressure, σ'_c. As the strain rate is constant, plots of strain versus time and strain rate versus time of a typical test would be the following:

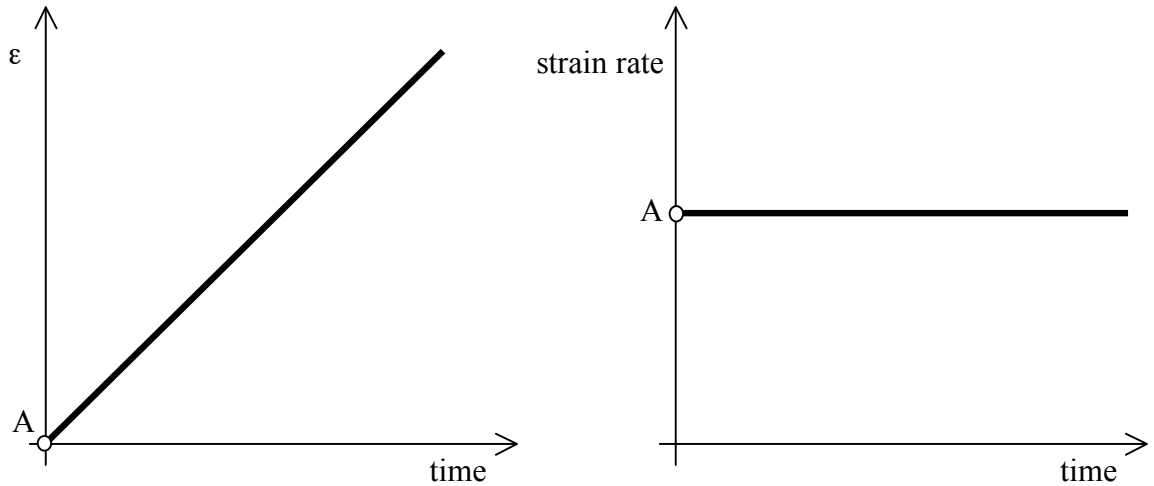

Figures 37 and 38 – Plots of strain x time and strain rate x time for constant rate of strain test

It is important to note that at the beginning of the test, at point A of the above plots, although the strain is zero, the strain rate is not zero. Therefore, as both strain rate and void ratio remains constant throughout the shearing phase, the viscous resistance would be fully mobilized at the start of the test and would remain constant throughout

the entire test (assuming that the coefficient of viscosity, $\eta(e)$, is independent of the shear strains).

On the other hand, as the frictional resistance is assumed to be a function of the shear strain only and as the clay is assumed to be normally consolidated, it would increase from zero (for $\varepsilon = 0$) at the beginning of the test to a maximum value at failure for a given shear strain, ε_f.

The resultant deviatoric stress x strain curve is obtained combining the viscous and the frictional resistances. As the viscous resistance is instantaneously mobilized, the initial part of the stress-strain curve would be a vertical line coinciding with the deviatoric stress axis. From this point on, the frictional resistance is mobilized, from zero for shear strain equal to zero to a maximum value at failure, for strain equal to ε_f. The following plot illustrates the deviatoric stress x strain curve for two tests consolidated to the same consolidation pressure but sheared with two different strain rates.

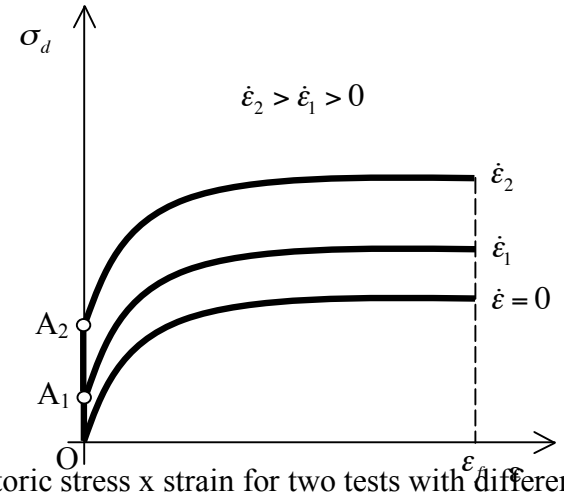

Figure 39 – Deviatoric stress x strain for two tests with different strain rates.

The curve with strain rate equal to zero is the curve that would be obtained provided a test specimen consolidated to the same consolidation pressure as the other two tests and with strain rate equal to zero could be carried out. For this curve, as the strain rate is null, no viscous resistance exists, and therefore all resistance is of frictional nature. The instantaneous mobilization of viscosity for tests with strain rates $\dot{\varepsilon}_1$ and $\dot{\varepsilon}_2$ are represented in the figure by segments OA_1 and OA_2, respectively. The deviatoric stress x strain curve for strain rate equal to zero is similar in concept to the zero strain rate compression curve and to the K_0 with zero strain rate (K_{0s}). They all represent the component of the behavior of the material that does not depend on the strain rate.

The behavior of the pore-pressure would be similar to the behavior of the frictional resistance, that is to say that the pore-pressure increases from zero (for $\varepsilon = 0$) at the beginning of the test to a maximum value at failure for a given shear strain. As the pore-pressure is assumed to be independent of the strain rate, any test, irrespective of the strain rate with which was carried out would develop the same pore-pressure curve. Therefore, for the tests with strain rates $\dot{\varepsilon}_1$ and $\dot{\varepsilon}_2$ represented above, the following unique pore-pressure x strain curve would be obtained.

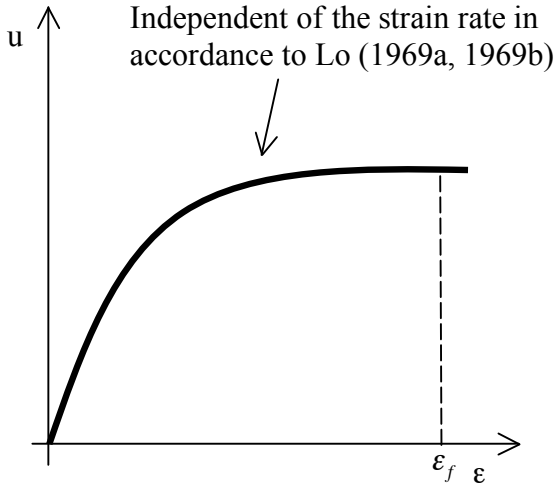

Figure 40 – Pore-pressure development during shear

The hypothesis of the pore-pressure as an unique function of strain is consistent with the proposition and findings of Lo (1969a, 1969b) and the observation of Lacerda (1976). However, other investigators such as Richardson (1963), Richardson and Whitman (1963), Ladd et al (1972), Hight (1982), Berre and Bjerrum (1973) and others, as shown in Sheahan et al (1996), have observed an increase in pore-pressure during shear with the decrease in strain rate. In this regard, it is believed in the present work that the increase in pore-pressure during shear with decreasing strain rate is related to the arrest of secondary consolidation as observed by Arulanandan et al (1971).

This increase of pore-pressure with time will also be addressed in this paper after the next section.

The mechanism of the Stress Relaxation test under triaxial conditions

In general a stress relaxation carried out in the triaxial apparatus begins as a regular consolidated undrained triaxial test sheared at a given strain rate and after a given strain is reached the triaxial press is stopped. From this point on, the specimen is maintained approximately at a constant strain state while the stress decays with time.

According to Martins's model, if the rigidity of the system were infinite, the stress decay would have to be instantaneous. However this does not happen and the stress decay occurs in time. Having in mind the edometric case it is possible that the stress relaxation under triaxial conditions occurs in time because of the rigidity of the system as well.

As in the edometric case, follows that the deviatoric stress can be written as:

$$\left(\sigma_1 - \sigma_3\right) = \left(\sigma'_{1s} - \sigma'_{3s}\right) + \left(\sigma'_{1v} - \sigma'_{3v}\right) \qquad \text{(10 bis)}$$

Assuming that the solid deviatoric stress can be represented by (without implying elastic behavior):

$$\left(\sigma'_{1s} - \sigma'_{3s}\right) = \sigma_{dsA} + E \cdot \varepsilon = \sigma_{dsA} + E \cdot \left(x_s / H_s\right) \tag{40}$$

Where:

σ_{dsA} is the solid effective stress at the beginning of the stress relaxation test;
E is a modulus (assumed to be constant within a stress range);
x_s is the vertical displacement experienced by the soil specimen; and
H_s is the height of soil specimen.

And that the viscous stress difference can be written as:

$$\left(\sigma'_{1v} - \sigma'_{3v}\right) = K \cdot \dot{\varepsilon}^n = K \cdot \left(\dot{x}_s / H_s\right)^n \tag{41}$$

Equation (10) be re-written as:

$$\left(\sigma_1 - \sigma_3\right) = \sigma_{dsA} + E \cdot \left(x_s / H_s\right) + K \cdot \left(\dot{x}_s / H_s\right)^n \tag{42}$$

Considering also that the rigidity of the system is such that is can be represented by:

$$F = k \cdot x_s \tag{43}$$

The deviatoric stress applied to the soil specimen can be represented by:

$$\left(\sigma_1 - \sigma_3\right) = \sigma_{dA} - k \cdot x_s / A_s \tag{44}$$

Where:

A_s is the area of the cross section of the soil specimen; and
σ_{dA} is the initial deviatoric stress at the beginning of the stress relaxation.

Therefore the differential equation of the "imperfect" stress relaxation process under triaxial conditions is:

$$\sigma_{dA} - k \cdot x_s / A_s = \sigma_{dsA} + E \cdot \left(x_s / H_s\right) + K \cdot \left(\dot{x}_s / H_s\right)^n \tag{45}$$

Equation (45) is similar to Equation (29) developed for the "imperfect" stress relaxation process under edometric conditions.

For $t = 0$, at the beginning of the "imperfect" stress relaxation process follows that $x_s = 0,\ F = 0$ and $\dot{x}_s = H_s \cdot \left[\frac{\sigma_{dA} - \sigma_{dsA}}{K}\right]^{\frac{1}{n}}$. Using the new auxiliary functions below:

$$A = \left(\sigma_{dA} - \sigma_{dsA}\right),\ B = \frac{k}{A_s},\ C = \frac{E}{H_s},\ B' = \left(C + B\right) \text{ and } D = K \cdot \left(\frac{1}{H_s}\right)^n$$

Follows that the solution of the differential equation is Equation (30) reproduced below:

$$x_s(t) = \left(\frac{A}{B'}\right) - \left(\frac{D}{B'}\right) \cdot \frac{1}{\left[\left(\frac{D}{A}\right)^{\left(\frac{1-n}{n}\right)} + \left(\frac{1-n}{n}\right)\frac{B' \cdot t}{D}\right]^{\left(\frac{n}{1-n}\right)}} \qquad \text{(30 bis)}$$

And the expression for the rate of displacement is also Equation (31) reproduced below as well:

$$\dot{x}_s = \frac{1}{\left[\left(\frac{D}{A}\right)^{\left(\frac{1-n}{n}\right)} + \left(\frac{1-n}{n}\right) \cdot \frac{B' \cdot t}{D}\right]^{\left(\frac{1}{1-n}\right)}} \qquad \text{(31 bis)}$$

Also, the stress decay function shown below will be similar to Equation (33):

$$\sigma(t) = \sigma_{dsA} + C \cdot \left\{ \left(\frac{A}{B'}\right) - \left(\frac{D}{B'}\right) \cdot \frac{1}{\left[\left(\frac{D}{A}\right)^{\left(\frac{1-n}{n}\right)} + \left(\frac{1-n}{n}\right)\frac{B' \cdot t}{D}\right]^{\left(\frac{n}{1-n}\right)}} \right\} + D \cdot \left\{ \frac{1}{\left[\left(\frac{D}{A}\right)^{\left(\frac{1-n}{n}\right)} + \left(\frac{1-n}{n}\right) \cdot \frac{B' \cdot t}{D}\right]^{\left(\frac{n}{1-n}\right)}} \right\} \qquad (46)$$

Where t is the time since the beginning of the stress relaxation process.

The second term to right of the equal sign in Equation (46) is the variation in the solid component of the deviatoric stress that occurs during the process. The last term to the right of the equal sign in Equation (46) is the stress decay in the viscous component of the deviatoric stress.

Substituting $t = 0$ in Equation (46) follows that:

$$\sigma'(0) = \sigma_{dA} \qquad (47)$$

Which is the initial stress condition at the beginning of the "imperfect" stress relaxation process and is independent of the rigidity of the system. Evluating the limit when $t \to \infty$ in Equation (46) follows that:

$$\lim \sigma'(t)_{t \to \infty} = \sigma_{dsA} + \left(\frac{E}{H_s}\right) \cdot \left(\frac{\sigma_{dA} - \sigma_{dsA}}{\frac{E}{H_s} + \frac{k}{A_s}} \right) \qquad (48)$$

If the system were "perfectly" rigid, which no actual system is, the process would be instantaneous. The effect of the rigidity of the system can be assessed by making all the other variables constant and varying k on Equation (46). The greater the rigidity

the faster the process. Making $k \to \infty$ on Equation (48) yields $\sigma' = \sigma_{dsA}$, which is in accordance to the model.

The equations above can be used for predicting the "imperfect" stress relaxation process provided the viscous and solid components of the effective stress as well as the rigidity of the system are known.

It is worth noting that because the differential equation was developed in terms of deviatoric stresses the pore-pressure does not influence the process and need not to be accounted for.

As there is no stress relaxation campaign in the published literature where all the elements required for making predictions can be assessed, no prediction could be made at the moment to assess the validity of the proposed equations. However, a preliminary check can be made by using Equation (31) and Test 26 carried out by Taylor (1955) in the same way the comparison for the rate of displacement x time plot was made for the available data from Garcia (1996).

This is only possible because Taylor used a proving ring and measured displacement as well as force during the stress relaxation. The data presented in the figure below comes from Figure 17 of Taylor (1955).

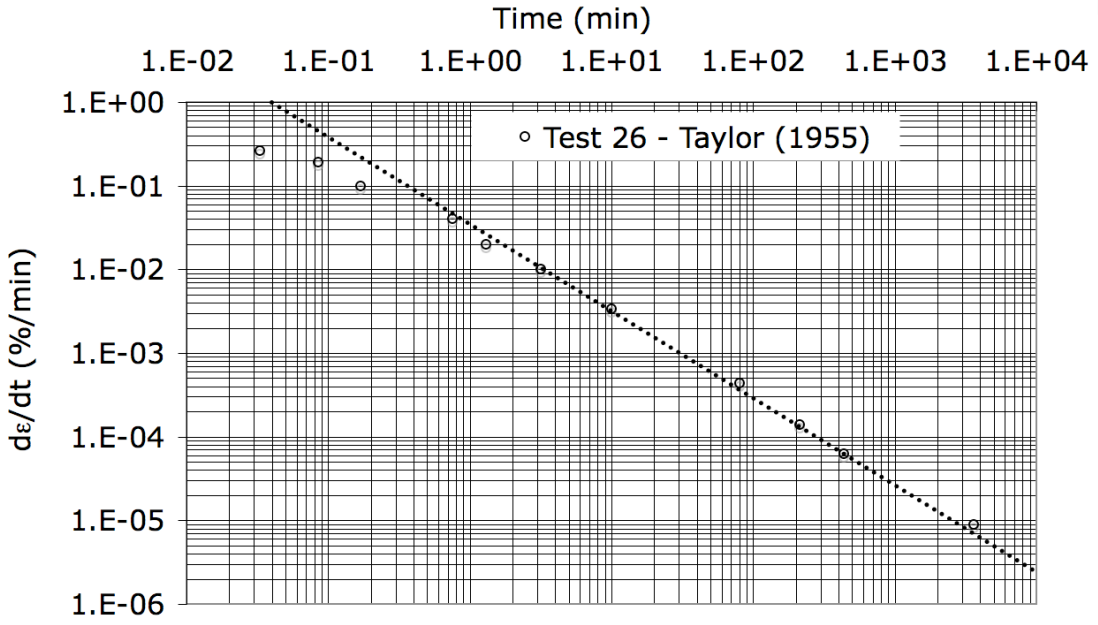

Figure 41 – Stain rate x time plot for Test 26 carried out by Taylor (1955).

As can be seen on the figure above the strain rate x time curve when plotted in a bi-log scale presents itself initially slightly convex and the later portion of the plots is approximately linear. Fitting a straight line through the 8 last points as shown by the dashed line in Figure 41, it is possible to calculate the value of n. As the slope of this line is about -1.05, n can be assessed to be about 0.048. This n value however should be considered as an exercise only, as it was assessed based on a single stress relaxation test that lasted for less than about 4,000 minutes.

As this test is the only that can provide some data that can be interpreted in the light of the concepts presented in this paper, it is premature to present conclusions about the applicability of the model regarding stress relaxation under triaxial conditions. The only conclusion that can be made is that the strain rate x time curve has a similar shape as Equation (31) and therefore the model may also be able to explain the stress relaxation under triaxial conditions.

In order to better investigate the applicability of the proposed equations is necessary to carry out more stress relaxation tests where the rigidity of the system is assessed and the displacements of the specimen during the process are measured.

One may argue that the system rigidity should be as high as possible in order to approximate the tests conditions to the theoretical condition of the "perfect" stress relaxation condition. By doing so, although getting closer to the perfect condition, the ability to measure accurately the stress decay decreases with increasing rigidity. In addition, no real structure/material have infinite rigidity, and because of this reason, the "imperfect" stress relaxation can be seen as more representative of an actual engineering problem.

The tests also need to last longer in order to observe if the last portion of the deviatoric stress x time plot is concave and asymptotic to a limiting (stationary) value as predicted by the equations.

Stress Relaxation Under Hydrostatic Conditions

Stress relaxation tests as the ones carried out by Arulanandan et al (1971), Holzer et al. (1973), Thomasi (2000), Dos Santos (2006) and Lima (1993) may also be interpreted using the framework of the model developed by Martins (1992) as modified by Alexandre (2000).

As mentioned in the previous sections, it is suspected that the rigidity of the system is responsible for the stress relaxation to occur through time. The comparison of the predictions and the test data carried by Garcia (1996) and the strain rate x time curve of Test 26 carried by Taylor (1955) support this tentative conclusion.

Having this in mind, it is possible that the stress relaxation under hydrostatic conditions may be due to the effect of the rigidity of the system. In this case, however, the responsible may be the water that fills the voids of the soil as it will be explained below.

The hydrostatic stress relaxation test as carried by Arulanandan et al. (1971) have two stages. The first state is the hydrostatic consolidation and the second stage is the closing of the drainage line and the observation of the pore-pressure build-up with time.

If, after the "end" of primary consolidation, the drainage line was not closed, the soil would be allowed to undergo secondary (hydrostatic) consolidation and the process would end in the same way the edometric secondary consolidation in accordance to the model ends: by transferring the viscous component entirely to the solid component of the effective stress and reaching the zero strain rate hydrostatic

compression line. However, when the drainage is closed, the viscous component cannot transfer to the solid component and nor can it transfer to the total stress, which is held constant. Therefore the viscous component of the hydrostatic effective stress has to be transferred to the pore-pressure.

In detail the process would be the following:

After the "end" of primary consolidation, the excess pore-pressure is approximately zero and the soil is undergoing secondary consolidation at an ever decreasing strain rate until, in accordance to Martins's model, the process stop at the zero strain rate line (the end of secondary consolidation line). Therefore, if the drainage is closed at a point in time after the "end" of primary consolidation, having the soil specimen a volumetric strain rate just before that, the soil will posses a viscous hydrostatic component of the effective stress.

After the drainage is closed, the volumetric strain rate has to drop to zero immediately and so the viscous hydrostatic component. As the total stress is held constant it cannot increase in time. On the other hand, because the solid component of the effective stress is a function of the void ratio this component cannot change as well. Therefore the pore-pressure has to increase to the same magnitude of the viscous component of the hydrostatic effective stress at the moment the drainage is closed.

Again, according to Martins's model (1996), the normal effective stress decay (and the pore-pressure build-up) is predicted to be instantaneous, what does not occur. Therefore, for the pore-pressure to build-up in time, in accordance to the mechanisms developed for the edometric and triaxial stress relaxation process, there must be some rigidity in the system that makes the process develop through time. It is suspected that the compressibility of the water is responsible for this effect.

Considering that the build up in pore-pressure is related to the change in the volume of water as below:

$$\Delta u = \frac{\Delta v_w}{v_0 \cdot n_s \cdot C_w} = \frac{\varepsilon_{vol}}{n_s \cdot C_w} \tag{49}$$

Where:

Δu is the variation in pore-pressure;
Δv_w is the variation in the volume of water;
v_0 is the initial volume of the soil specimen before closing the drainage;
$\varepsilon_{vol} = \frac{\Delta v_w}{v_0}$ is the volumetric strain under undrained conditions.
n_s is the porosity of the soil specimen; and
C_w is the compressibility of the water that fills the voids of the soil specimen.

Considering also that the change in the solid hydrostatic component of the effective stress is proportional to the change in volume of the soil specimens as below:

$$\Delta\sigma'_s = \frac{\Delta v}{v_o \cdot C_{ss}} \tag{50}$$

Where:

$\Delta\sigma'_s$ is the variation in the solid hydrostatic component of the normal effective stress;
Δv is the variation in the volume of the soil specimen;
v_0 is the initial volume of the soil specimen before the closing of the drainage; and
C_{ss} is the compressibility of the soil specimen.

And that the equation that relates total stress, effective stress with its two components (the solid and viscous components) and the pore-pressure can be expressed by:

$$\sigma = \sigma'_s + \sigma'_v + u \tag{51}$$

The differential equation of the hydrostatic stress relaxation process can be represented by:

$$\sigma = \frac{\Delta v}{v_o \cdot C_{ss}} + K \cdot \dot{\varepsilon}_{vol}^{n} + \frac{\Delta v_w}{v_0 \cdot n_s \cdot C_w} \tag{52}$$

Where the viscous hydrostatic component of the effective stress can be represented by a power law of the volumetric strain rate, $\dot{\varepsilon}_{vol}$. Assuming that the very small variation in volume of the soil specimen (under undrained conditions) is due to the equally small variation in volume of the water under the excess pore-pressure u, follows that Equation (52) can be re-written as:

$$\sigma = \left[\frac{1}{C_{ss}} + \frac{(e+1)}{e \cdot C_w}\right] \cdot \varepsilon_{vol} + K \cdot \dot{\varepsilon}_{vol}^{n} \tag{53}$$

Where:

e is the void ratio; and
$\varepsilon_{vol} = \frac{\Delta v_{ss}}{v_0} = \frac{\Delta v_w}{v_0}$ is the volumetric strain under undrained conditions.

The solution of Equation (53) is:

$$\varepsilon_{vol} = \left(\frac{\sigma - \sigma'_{si}}{E_{eq}}\right) - \left(\frac{K}{E_{eq}}\right) \cdot \frac{1}{\left[\left(\frac{K}{\sigma - \sigma'_{si}}\right)^{\left(\frac{1-n}{n}\right)} + \left(\frac{1-n}{n}\right)\frac{E_{eq} \cdot t}{K}\right]^{\left(\frac{n}{1-n}\right)}} \tag{54}$$

Where:

$E_{eq} = \frac{1}{C_{ss}} + \frac{(e+1)}{e \cdot C_w}$ is the "equivalent" deformation modulus; and

σ'_{si} is the initial value of the solid hydrostatic component of the normal effective stress at the moment of closing the drainage.

The strain rate expression for the hydrostatic case is:

$$\dot{\varepsilon}_{vol} = \frac{1}{\left[\left(\frac{K}{\sigma - \sigma'_{si}}\right)^{\left(\frac{1-n}{n}\right)} + \left(\frac{1-n}{n}\right) \cdot \frac{E_{eq} \cdot t}{K}\right]^{\left(\frac{1}{1-n}\right)}} \tag{55}$$

Equations (54) and (55) are the expressions of the volumetric strain and volumetric strain rate versus time and are similar to the displacement and rate of displacement versus time expressions of the previous triaxial and edometric cases.

Considering that $\varepsilon_{vol} = \frac{\Delta v_{ss}}{v_0} = \frac{\Delta v_w}{v_0}$, the expression of the pore-pressure build-up in time, obtained from combining Equations (54) and (49), is given below:

$$u = \left[\frac{(e+1)}{e \cdot C_w}\right] \cdot \left\{ \left(\frac{\sigma - \sigma'_{si}}{E_{eq}}\right) - \left(\frac{K}{E_{eq}}\right) \cdot \frac{1}{\left[\left(\frac{K}{\sigma - \sigma'_{si}}\right)^{\left(\frac{1-n}{n}\right)} + \left(\frac{1-n}{n}\right)\frac{E_{eq} \cdot t}{K}\right]^{\left(\frac{n}{1-n}\right)}} \right\} \tag{56}$$

Typical plots of pore-pressure build-up in time according to the Equation (56) with arithmetic and log scales for the time axis are presented below:

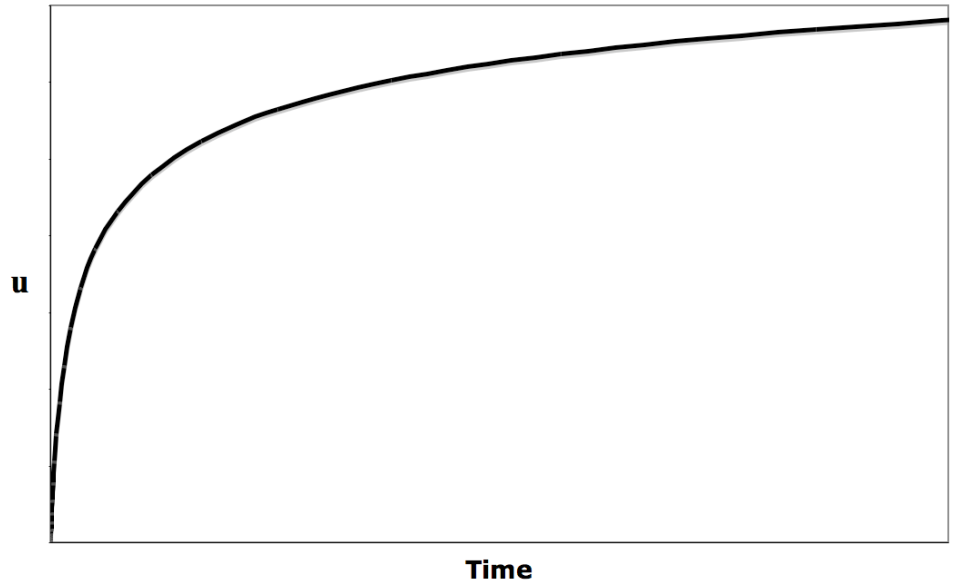

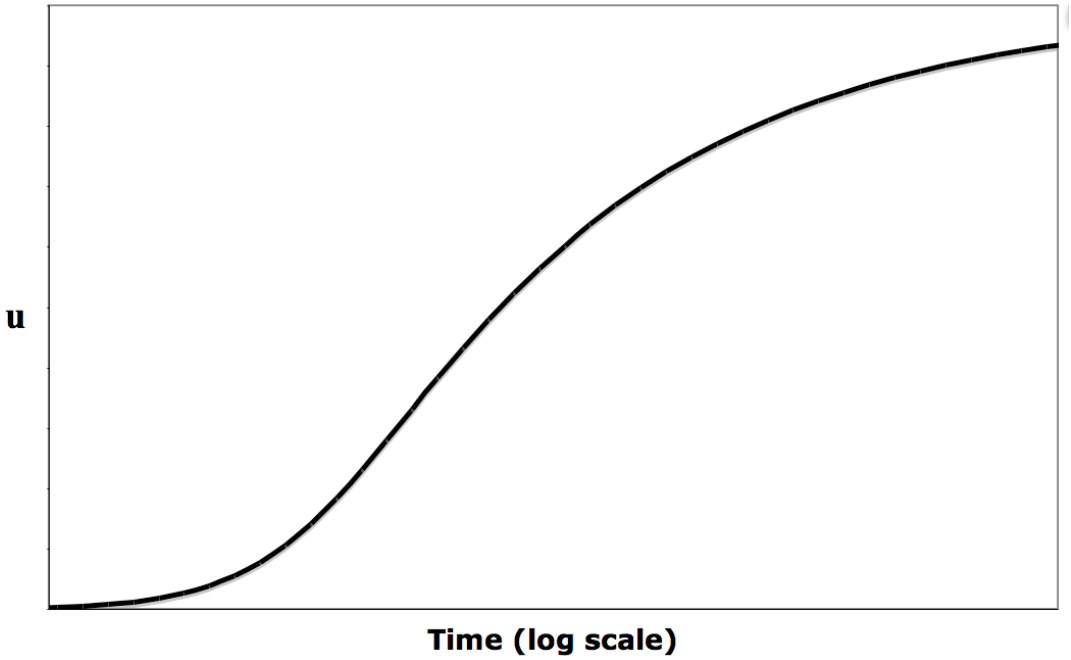

Figures 42 and 43 – Pore-pressure build-up x time in arithmetic and log scales.

The plots presented in Figures 42 and 43 are similar to Figures (15) and (16) for the strain x time plot of the creep process.

Equation (56) could be used to predict pore-pressure build-up in time provided the viscous and solid components of the hydrostatic effective stress as well as the compressibility of the water are known. However, considering the published tests available in the technical literature, in addition to the lack of information that could be used for deriving the required parameters, the following three difficulties arise:

- The assessment of the compressibility of the water: As shown in Fredlund (1976), the compressibility of the water containing only 1% of dissolved gas is 3 orders of magnitude less than the compressibility of the water with no dissolved gas;
- Non-uniformity of the viscous normal effective stress after consolidation: After the "end" of primary consolidation when the drainage is closed, there will be a distribution of void ratio across the sample, where smaller void ratios are expected near the drainage frontier and greater void ratios as expected at the "undrained" axis (case of cylindrical specimens) or plane. In addition, the strain rates will also vary across the specimen when the drainage is closed and therefore it is likely that the viscous effective stresses are unevenly distributed across the specimen. As the pore-pressure has to be the same everywhere in the specimen when the stationary pore-pressure is reached, it is expected that the build-up process will be even more delayed the greater the dispersion of the "local" viscous component is in relation to the average or "global" viscous component; and
- The occurrence of diffusion: Diffusion of water through the latex membrane occurs due to the difference in water pressure on opposite sides of the membrane.

The last of the difficulties may be overcome by using “mercury jackets”/”mercury sleeves” or the like. The effects of the second difficulty listed above may be reduced by making two build-up stages. The first stage is expected to last considerably more than the second, as after the first stage, the viscous component of the effective stress is likely more evenly distributed. The first difficulty is, however, the more problematic, as with a quantity of dissolved gas as little as 1% the compressibility of the water drops 3 orders of magnitude.

Because of the reasons explained above, predictions of the pore-pressure build-up may be very difficult to make. Despite of this, a check similar to the one done for Tests 26 carried out by Taylor (1955) can be made.

Although the measurement of the change in volume expected for the water during the pore-pressure build-up is not feasible, the rate of increase in pore-pressure may be used for this matter.

As can be seen on Equation (49) the build-up in pore-pressure is directly proportional to the volumetric strain of the water under undrained conditions and inversely proportional to the porosity of the specimen and the compressibility of the water. Therefore, because of Equation (49), the volumetric strain rate is directly proportional to the rate of increase of pore-pressure in time. In other words, a plot of du/dt (log scale) *x time* (time in log scale) similar in shape to the plot of the variation of the *strain rate (or rate of displacement) x time* as represented by Figures 29 to 35 (the tests from Garcia, 1996) and Figure 41 (Test 26 from Taylor 1955) must exist for Equation (53) to be valid.

This was done for one test carried out for one by Arunalandan et al (1971) and another carried out by Holzer et al. (1973). These two tests were selected for this assessment as they were carried out using a mercury sleeve, which prevents the process of diffusion from occurring. They were also carried out on the same soil, the San Francisco Bay Mud.

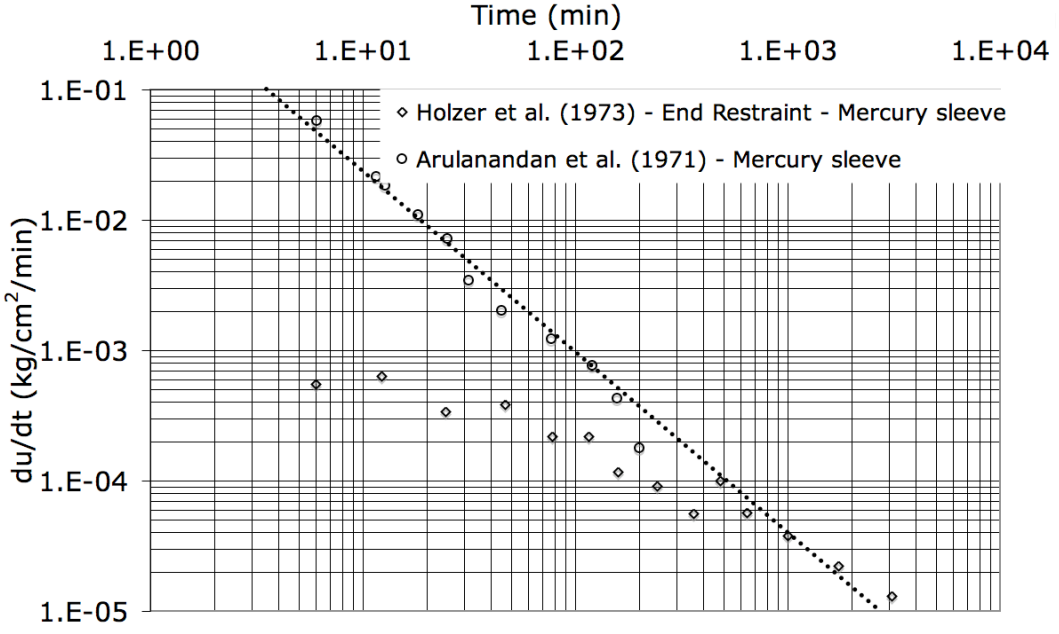

Figure 44 – Plots of du/dt (log scale) x time (log scale) for the tests carried out by Arunalandan et al (1971) and Holzer et al. (1973).

As can be seen, Figure 44 resembles Figure 14 corroborating the impression that the pore-pressure increase through time can be explained by the model proposed by Martins (1992) as modified by Alexandre (2006) when the "rigidity" of the system is taken into account (in this case is the inverse of the compressibility of the water).

As the compressibility of the water that fills the voids of the soil is expected to be similar for these tests carried on the San Francisco Bay Mud, it would be expected that the du/dt (log scale) x time (log scale) curves would line up one on "top" of the other as they did.

Furthermore, as the stabilized pore-pressure from the test carried out by Arunalandan et al. (1971) is greater than the one from the test carried by Holzer et al. (1973), it would be expected that the du/dt (log scale) x time (log scale) curve from Arulanandan et al. (1971) would be displaced along the "straight" line but would be higher than the curve from Holzer et al. (1973), as it did as well. Fitting a straight line as shown by the dashed line in Figure 44, it is possible to calculate the value of n. As the slope of this line is about -1.4, n can be assessed to be about 0.284. This n value however should be considered as an exercise only, as it was assessed based on two tests.

Despite of this agreement between the model and the experimental data, more hydrostatic and other undrained stress relaxation tests such as the ones mentioned in the previous sections are necessary for better assessing the applicability of the proposed equation. These tests are recommended to be designed to account for the possible problems listed in this section and are also recommended to last longer in order to better define the latter portion of the stress relaxation x time and pore-pressure variation x time plots.

Summary

In regard to the predictions made for the "imperfect" stress relaxation tests carried out by Garcia (1996) the following may tentatively be concluded:

- The power law function of the strain rate for representing the viscous component of the effective stress seams to fit well the experimental data;
- The stress relaxation process occurs through time because of the rigidity/compressibility of the system and because of the occurrence of creep;
- The predictions made agree reasonably well with the experimental data both qualitatively and quantitatively;

In regard to the model developed by Martins (1992) and the modification proposed by Alexandre (2006):

- The framework of the model is based on physical reasoning and allows for a unified approach for describing time-dependent processes such as creep and stress relaxation under various stress and drainage conditions;
- The zero strain rate lines (for edometric or hydrostatic and other lines) are the lines that limit the time-dependent processes. This concept, developed by

Martins, which was verified experimentally for several clays, allows for the prediction of limit pore-pressure increase and limit deformations in the soil mass putting an end to time-dependent processes;

- The creep and the "perfect" stress relaxation processes can be seen as particular cases of the general "imperfect" stress relaxation process. In this view, by making negligible the rigidity, the approximate creep process is obtained. By making infinite the rigidity, the "perfect" stress relaxation process is obtained. More importantly, the rigidity of the system, which is always present in actual engineering applications was considered and incorporated in analysis of time-dependent processes such creep and stress relaxation.

In regard to the conjectures developed in this paper:

- Two expressions for K_0 as a function of the viscous and solid components of the effective stress were developed. In the first equation, where no macroscopic lateral deformation is considered for the edometric compression, K_0 is expected to increase both during secondary consolidation and stress relaxation. In the second equation, where the microscopic deformation of the soil specimen under edometric compression is considered, K_0 is expected to decrease both during secondary consolidation and stress relaxation;
- The differential equations of the "imperfect" stress relaxation tests under triaxial and hydrostatic (undrained) conditions were obtained as well their respective solutions;
- Experimental data from Taylor (1955), Arulanandan et al. (1971) and Holzer et al. (1973) seem to corroborate the impression that the model proposed by Martins (1992) as modified by Alexandre (2006) can be applied for explaining the stress relaxation under triaxial and hydrostatic conditions;

Despite of the promising preliminary assessment carried out for the proposed equation for the triaxial and hydrostatic stress relaxation processes, more, longer and specially designed stress relaxation tests are required for a better assessment of the validity of the proposed equations. The basic requirements of these tests were outlined in this paper.

References

Adachi T., Okano M., (1974), A constitutive equation for normally consolidated clay, Soils and Foundations, 14, (4), 55-73.

Aguiar V. N., (2008), Consolidation Characteristics of the clay from the channel of Santos's Port, Barnabé Island region. M.Sc. thesis, COPPE/UFRJ, Rio de Janeiro, Brazil (in Portuguese)

Akai, K., Adachi, T., & Ando, N. (1975), Existence of a unique stress-strain-time relation of clays. Soils and Foundations 15, No. 1, 1-16.

Alexandre (2000), The Undrained Creep According to Martins's Model (1992), M.Sc. thesis, COPPE/UFRJ, Rio de Janeiro, Brazil (in Portuguese)

Alexandre (2006), Contribution to the Understanding of the Undrained Creep, Ph.D. thesis, COPPE/UFRJ, Rio de Janeiro, Brazil (in Portuguese)

Anderson, O. B. and Douglas, A. G. (1970), Bonding, Effective Stresses and Strength of Soils, J. Soil Mech. Found. Div., Proc. Am. Soc. Civ. Eng. 96:1073-1077

Andrade, M. E. S., (2009), Contribution to the Study of Soft Clays from the City of Santos. M.Sc. thesis, COPPE/UFRJ, Rio de Janeiro, Brazil (in Portuguese)

Arulanandan, K., Shen, C. K., and Young, R. B. (1971). Undrained creep behaviour of a coastal organic silty clay. Géotechnique, 21(4), 359-375.

Berre T., and Bjerrum L., (1973). Shear strength of normally consolidated clays. Proc. 8th Intl. Conf. on Soil Mech. And Found. Eng. Vol 1 pp 39–49.

Bishop, A.W. & Lovenbury, H.T. 1969, Creep characteristics of two undisturbed clays, Proc. 7th ICSMFE, Mexico, Vol. I, pp. 29-37.

Bjerrum, L. (1967). Engineering geology of Norwegian normally consolidated marine clays as related to settlement of buildings. Geotechnique 17, No. 2, 81 – 118. 230 – 247.

Bjerrum, L., Simons, N., and Torblaa, I., (1958). The effect of time on the shear strength of soft marine clay." Proc., Brussels Conf. on Earth Pressure Problems, Vol. 1, 148–158.

Campanella, R. G., (1965), Effect of Temperature and Stress on the Time-Deformation Behaviour of Saturated Clay," PhD Dissertation, University of California, Berkeley.
Christensen, R. W., and T. H. Wu, (1964), analysis of Clay Deformation as a Rate Process, J. Soil Mech. Found eng. Div., ASCE, vol. 90, no. SM6, pp. 125-157.

Dos Santos, R. M., (2006), Experimental Study of a Viscous Parcel on the Normal Effective Stress of a Clayey Soil. M.Sc. thesis, COPPE/UFRJ, Rio de Janeiro, Brazil (in Portuguese)

Feijó, R. L., (1991) Relationship Between Secondary Compression, Over Consolidation Ratio and the At-rest Earth Pressure Coefficient. M.Sc. thesis, COPPE/UFRJ, Rio de Janeiro, Brazil (in Portuguese)

Fredlund, D. G., (1976). Density and compressibility characteristics of air-water mixtures". Canadian Geotechnical Journal, 13(4), 386-396.

Garcia, S. G. F., (1996) Relationship Between Secondary Consolidation and Stress Relaxation of a soft clay,M.Sc. thesis, COPPE/UFRJ, Rio de Janeiro, Brazil (in Portuguese)

Glasstone, S., Laidler, K. J., & Eyring, H., 1940, Theory of Rate Processes. First Edition, New York: McGraw-Hill Book Co.

Hicher, P. Y. (1988), The Viscoplastic Behavior of Bentonite, in Rheology and Soil Mechanics, M. J. Keedwell (ed.), London: Ensevier, pp. 89-107.

Hight, D. W., (1983), Laboratory Investigation of Sea Bed Clays, Ph.D. thesis, Imperial College, London, UK.

Holzer, T.L., Hoeg, K., and Arulanandan, K. ,1973, Excess pore pressures during undrained clay creep. Can. Geotech. J. 10(1), pp. 12-24.

Kavazanjian, E. and Mitchell, J. K., (1984), Time Dependence of Lateral Earth Pressure, Journal of Geotechnical Engineering, ASCE;110(4):530-533

Kavazanjian, E., Mitchell, J. K., (1984), Time dependence of lateral earth pressure, Journal of Geotechnical Engineering - ASCE 1984;110(4):530-533.

Kutter, B.L., and Sathialingam, N., (1992), Elastic–viscoplastic modelling of the rate-dependent behaviour of clays. Géotechnique, 42(3): 427–441.

Lacerda, W. A. &Houston, W. N. (1973). Stress relaxation in soils, Proc. 8th ICSMFE Vol. 1, 221–227.

Ladd, C. C., Williams, C. E., Connell, D. H., and Edgers, L., (1972), Engineering Properties of Soft Foundation Clays at two Louisiana Levee Sites, Res. Rep. R72-26< Massachusetts Inst. Of Technol., Cambridge, Massachusetts.

Ladd, C. C., and R. Foot, New Design Procedure for Stability of Soft Clays, J. Geotech. Eng. Div., ASCE, vol. 100, no. GT7, 763-786, 1974.

Leroueil, S., Kabbaj, M., Tavenas, F., and Bouchard, R., (1985), Stress-strain-strain rate relation for the compressibility of sensitive natural clays." Geotechnique, 35(2), 159-180.

Lima, G. P., (1993), Study of a Non-Linear Theory for One-dimensional Consolidation, ,M.Sc. thesis, COPPE/UFRJ, Rio de Janeiro, Brazil (in Portuguese)

Lo, K. Y., (1969a), The pore pressure – strain relationship for normally consolidated undisturbed clays, Part I Theoretical considerations. Canadian Geotechnical Journal 6(4): 383-394.

Lo, K. Y., (1969b), The pore pressure – strain relationship for normally consolidated undisturbed clays, Part II Experimental Investigation and practical application. Canadian Geotechnical Journal 6(4): 395-412.

Martins, I. S. M., (1992), Fundamentals of a Behavioral Model for Saturated Clayey Soils, Ph.D. thesis, COPPE/UFRJ, Rio de Janeiro, Brazil (in Portuguese)

Martins, I. S. M., Santa Maria, P. E. L. S., Lacerda, W. A., Santa Maria, F. C. M. S., Alexandre, G. F., Thomasi, L., Guimaraes, P. F., (2001), Fundamentals of a

Behavioural Model of Saturated Clays, In: Encontro Propriedades de Argilas Moles Brasileiras, 2001, Rio de Janeiro, v. 1. p. 50-78 (in Portuguese).

Mesri, G., Febres‐Cordero, Shields, E., D. R., and Castro A., (1981), Shear Stress‐Strain--Time Behavior of Clays, Géotechnique, 31, 4 pp. 537‐552.

Mitchell, J. K., 1964, Shearing resistance of soils as a rate process. Journal of the Soil Mechanics and Foundations Division, ASCE, 90(1): 29–61.

Murayama, S. and Shibata, T., (1958), On the rheological characters of clay. Disaster Prevention Research Institute, Kyoto University, Bulletins, Bulletin No. 26, pp. 1-43.
Murayama, S. & Shibata, T. (1961), Rheological properties of clays, Proc. 5th ICSMFE, Vol. I, pp. 269-273.

Murayama, S., and Shibata, T., (1964) Flow and stress relaxation of clays Proceedings of I UTAM T Symposium on Rheology and Soil Mechanics, Grenoble Springer Verlag pp. 99-129.

Murayama, S., Sekiguchi, H., and Ueda, T., (1974), A Study of the Stress-Strain-Time Behavior of Saturated Clays Based on a Theory of Nonlinear Viscoelasticity, Soil and Foundations, Vol. 14, No. 2, pp 19-33.

Richardson, A. M., (1963), The relationship of the effective stress-strain behaviour of a saturated clay to the rate of strain, ScD thesis, Massachusetts Institute of Technology, Cambridge, Massachusetts

Richardson, A. M. and Whitman, R. V., (1963). Effect of strain-rate upon undrained shear resistance of a saturated remoulded fat clay. Géotechnique. Vol. 13, No.4, pp. 310-324.

Saada, A. S., (1962), A Rheological Analysis of Shear and Consolidation of Saturated Clays, Highway Research Board Bulletin 342, pp. 52-76.

Santa Maria, F. C. M., (2002), Rheological experimental study of the coefficient of earth pressure at rest, K_0, Ph.D, thesis, COPPE/UFRJ, Rio de Janeiro, Brazil (in Portuguese)

Santa Maria, P. E. L., Martins, I. S. M., and Santa Maria, F. C. M., (2010), Rheological behaviour os soft clays, 2nd International Symposium on Frontiers in Offshore Geotechnics

Santa Maria et al. (2012)

Schmertmann, J. H., (1983), A simple question about consolidation, J. Geotech. Engrg., ASCE, 109(1), 119 – 122.

Sekiguchi, H., (1984), Theory of undrained creep rupture of normally consolidated clay based on elasto- viscoplasticity, Soils and Foundations Vol. 24, No. 1, pp. 129- 147, Japanese Society of Soil Mechanics and Foundation Engineering.

Sheahan, T. C., Ladd, C. C., and Germaine, J. T. 1996. "Rate dependent undrained shear behavior of saturated clay." J. Geotech. Engrg., 1222, 99–108.

Sheahan, T. C. and Kaliakin, V.N. (1998). "Integrating Micromechanics in Modeling Relaxation Behavior of Cohesive Soils," Proceedings of the Biot Conference on Poromechanics, Université Catholique de Louvain, Louvain-la-Neuve, Belgium, Balkema, 147-152.

Silvestri, V., Soulie, M., Touchan, Z., and Fay, B. 1988. Triaxial relaxation tests on a soft clay. In Advanced triaxial testing of soil and rock. ASTM STP 977. Edited by R.T. Donaghe, R.C. Chaney, and M.L. Silver. American Society for Testing and Materials, Philadelphia, Pa. pp. 321–337.

Taylor, D. W., and Merchant, W., (1940), Theory of Clay Consolidation accounting for Secondary Compressions, reprinted from Journal of Mathematics and Physics, Vol. XIX, No. 3, July 1940

Taylor, D. W., (1942), Research on Consolidation of Clays, Serial 82, Massachusetts Institute of Technology, Cambridge, Massachusetts.

Taylor, D. W., (1943), Cooperative Research on Stress, Deformation and Strength Characteristics of Soils, Submitted from the Soil Mechanics Laboratory, Mass. Institute of Technology to the Waterways Experiment Station; 1940 to 1944, Report #9.

Taylor, D. W., (1955), Review of Research on Shearing Strength of Clay, Submitted from the Soil Mechanics Laboratory, Mass. Institute of Technology to the Waterways Experiment Station.

Terzaghi, K., (1941), Undisturbed Clay Samples and Undisturbed Clays, Journal of the Boston Society of Civil Engineers, Vol. 28, No. 3, pp. 211-231.

Thomasi, L., (2000), About the Existance of a Viscous Parcel on the Normal Effective Stress, M.Sc. thesis, COPPE/UFRJ, Rio de Janeiro, Brazil (in Portuguese)

Vaid, Y. P. &Campanella, R. G. (1977), Time-dependent behaviour of undisturbed clay, ASCEJ. Geotech. Engng103, No. 7, 693–709.

Walker, L.K., 1969. "Secondary Settlement in Sensitive Clays", Canadian Geotechnical Journal, Vol. 6, No2, pp. 219-222.

Wu, T. H., Douglas, A. G., Goughour, R. D., (1962), Friction and Cohesion of Saturated Clays, ASCE, JSMFD, Vol. 88, No. SM3, pp. 1-32.